UNIVERSITA' DI NAPOLI "FEDERICO II"

DOTTORATO DI RICERCA
BIOCHIMICA E BIOLOGIA MOLECOLARE E CELLULARE
XXIII CICLO

Poly(ADP-Ribose) Polymerase (PARP) signaling of DNA damage induced by Topoisomerase 1 (TOP1) inhibition in carcinoma cells:

chemotherapeutic implications of PARP and TOP1 inhibitors.

Candidate
Giovanna D'Onofrio

Tutor
Prof. Piera Quesada

Coordinator
Prof. Paolo Arcari

Academic Year 2010/2011

RINGRAZIAMENTI E DEDICHE

Mi sembra scontato ringraziare il gruppo REP che mi ha accolta nel suo laboratorio e mi ha permesso di svolgere la PARP ricerca!!! Di sicuro questi tre anni sono stati formativi dal punto di vista professionale: l'insuccesso o la gioia di un risultato ottenuto, la cura delle mie celluline, la determinazione nel riuscire ad affrontare mille imprevisti…, tante cose che nel mio piccolo mi han responsabilizzata e fatta crescere.

First of all, ringrazio la mia prof, *Piera Quesada*, non solo per avermi trasferito l'amore per la ricerca, ma per l'enorme affetto ricevuto (e altrettanto ricambiato) …; con la sua voce squillante, il rumore di chiavi ed il tacchettino..., inconfondibili segnali riconoscibilissimi che davano il tempo di poter occultare qualche magagna!!!

Vogliamo parlare di *Maria Malanga*? Una persona dolcissima, che con la sua calma mi ha rassicurata in ogni situazione, sia lavorativa che personale… un grandissimo punto di riferimento, per tutto!! .. e costretta a mille sobbalzi causati dalla porta sbattuta, senza maniglia, dello studiolo!!

…per non parlare di "*mamma" Me'*, che si è rivelata una grande amica, che mi ha trasferito tantissime nozioni e "supportata" in tantissime occasioni, ma che soprattutto mi ha coccolata sbucciandomi infinite mele e nutrendomi con dolci e rustici buonissimi!!! Il "pacco Mena" è stato comprensivo anche delle sue piccole, *Alessia* e *Fabiana*, ormai mie nipotine acquisite, che io stra-adoro e di cui non potrei più fare a meno.

Periodi bui, con "cappe ululanti" e interminabili blot (anche di pezzi di pomodoro) sono stati illuminati dalla presenza della mia pulc, *Mariateresa*, anche lei carissima amica, che con la sua lentezza, cavoli ammuffiti e frasi dislessiche, ha reso meno pesanti molte giornate dure e stressanti… dentro e fuori dal laboratorio!!! … inoltre, "creatrice" di Mr Wilson, il nostro supervisor (… accompagnato dalle urla della prof per l'uso improprio dei guanti e il consenso di Maria per riprodurlo ai suoi nipotini!!!).

Le mie "compagnelle di nullafacenza" , *Amalia (PZC)*, *Marianna, Mariella* e *Lidia*, complici di tante risate, sfilate per i corridoi e "dolcissimi" complimenti!!!!!!! … e i miei "schiavetti-tesisti", *Manuela, Irma, Susy ed Alessandro,* che nonostante il breve periodo trascorso insieme a lavoro sono sempre affettuosissimi !!

Ho trascorso romantiche visioni di comete con Cometina (*Valeria*), e "vacanze romane" con *Annalisa* e *Alessia* … le mie tre "collaboratrici", insieme al prof

Fulgione e la prof *Grazia Graziani*, che in un giorno gelido romano mi ha ripresa, con grande premura, per aver indossato un semplice smanicato.
Grazie alle trasferte romane, ho potuto riscoprire un forte legame con mia cugina *Leti*, che mi è molto vicina per tante cose … e che ha messo a disposizione il suo congelatore per ospitare il "topocano". Un ringraziamento speciale va anche a *zio Pep*, che mi considera "la sua scienziata" , un secondo padre e alla *nonna*, sempre piena di vita e che crede sempre tanto in me …e che con il suo "diabete obbediente" e furti di dolcini rende gioiosi tantissimi pranzi domenicali, e non solo ..!!
Simina, mia sorella acquisita, a cui voglio un bene infinito, che mi sopporta ormai da circa 15 anni, mia memoria storica (a volte distorta!!!) … che con i suoi attacchi ansiogeni e la sua vocina "soave" ha sempre spronato la mia flemma.
La mia cognatina, *Adri* … per fortuna mi è andata bene!!! … una preziosa amica ed il mio adorato fratello, Plu Plu (*Dario*), che riesce a capirmi anche senza parlare, ormai martorizzato da noi per la sua estrema golosità.
At the end, ultimi nomi (non per importanza).. al mio *papà*, che mi è vicino in un modo tutto speciale (che solo mio fratello conosce bene), e alla mia *mamma*, che vive a 360° ogni mio insuccesso e gioia … e seppur cane e gatto, siamo estremamente legate!!
Tutti i sopraelencati protagonisti sono i veri coautori del mio periodo di dottorato, cui segue un ulteriore periodo formativo … e come direbbe la prof: "Armiamoci e partite" per un nuovo tour de force!!!

SUMMARY

A novel molecular approach to enhance the antitumour activity of Topoisomerase 1 (TOP1) inhibitors relies on the use of chemical inhibitors of poly(ADP-ribose) polymerase (PARP). Poly(ADP-ribosyl)ation is involved in the regulation of several cellular process such as DNA repair, cell cycle progression and cell death. The molecular mechanism underlying tumor chemosensitization to TOP1 poisons by PARP inhibitors have been in part clarified by recent findings showing that poly(ADP-ribosyl)ated PARP-1 and PARP-2 counteract camptothecin action facilitating resealing of DNA strand breaks. Moreover, repair of DNA strand breaks induced by poisoned TOP1 is slower in the presence of PARP inhibitors, leading to increased toxicity.

In the present study, we compared the effects of the camptothecin derivative Topotecan (TPT) and the second-generation PARP inhibitor PJ34, administered as single agents or in combination, in cervix (HeLa) and breast (MCF7) carcinoma cells, both BRCA1/2$^{+/+}$ and p53$^{+/+}$.

The two cell lines gave similar results: (i) TPT-dependent cell growth inhibition and cell cycle perturbation were incremented by the presence of PJ34; (ii) higher levels of DNA strand breaks were found in cells subjected to TPT+PJ34 combined treatment; (iii) PARP-1 and -2 modification was evident in TPT-treated cells and was reduced by TPT+PJ34 combined treatment; (iv) concomitantly, a reduction of soluble/active TOP1 was observed. Likewise, PARP-1 shRNA HeLa cells showed increased TPT-dependent cytotoxicity and DNA damage in the presence of PJ34. Furthermore, TPT-dependent induction of p53 and p21 was found 24-72 h after treatment and PJ34 further increased p53 levels either in PARP-1 proficient and silenced cells. Finally, TPT-dependent

onset of the apoptosis was also incremented by PARP inhibitor as shown by the PARP-1 proteolysis, Bax and active-caspase 3 expression.

The characterization of such signaling network can be relevant to a strategy to overcome acquired TOP1-poisoned chemoresistance.

RIASSUNTO

Una nuova strategia molecolare che incrementa l'azione antitumorale degli inibitori della Topoisomerasi 1 (TOP1) si basa sull'utilizzo di inibitori delle poli(ADP-ribosio) polimerasi (PARP). La poly(ADP-ribosil)azione è una modifica post-traduzionale coinvolta nella regolazione di diversi processi come il riparo del DNA, la progressione del ciclo cellulare e la morte cellulare. Il meccanismo molecolare che sottende la chemiosensibilizzazione dei veleni di TOP1 in presenza degli inibitori di PARP è in parte spiegato dal fatto che PARP-1 e -2, in forma modificata, interagiscono con il complesso DNA-TOP1-inibitori di TOP1 promuovendo un rapido rilascio di TOP1 dal DNA. Inoltre, il riparo delle rotture sul DNA indotte dai veleni di TOP1 è meno efficiente in presenza degli inibitori di PARP, che incrementano quindi la citotossicità dell'agente chemioterapico.

Nel presente studio, abbiamo comparato gli effetti dell'inibitore di TOP1 Topotecano (TPT) e dell'inibitore di PARP PJ34, somministrati come singoli agenti o in combinazione in cellule di carcinoma della cervice uterina (HeLa) e della mammella (MCF7), entrambe BRCA1/2$^{+/+}$ e p53$^{+/+}$. Sono state anche analizzate cellule HeLa silenziate stabilmente per PARP-1 mediante siRNA (denominate HeLa^{SiP-1}).

Le due linee cellulari mostrano risultati simili: (i) l'inibizione della crescita cellulare e la perturbazione del ciclo cellulare indotte dal TPT sono incrementate in presenza del PJ34; (ii) alti livelli di danno al DNA sono stati riscontrati in seguito al trattamento combinato TPT+PJ34; (iv) l'attivazione di PARP-1 e -2 è stata evidenziata nelle cellule trattate con TPT e ridotta dall'aggiunta del PJ34. In particolare, le cellule HeLa^{SiP-1}

mostrano elevati livelli di danno al DNA ed una citotossicità maggiore, dipendente dal TPT, in presenza di PJ34.

E' stata inoltre riscontrata un'induzione dell'espressione di p53 e p21 TPT-dipendenti 24-72 h dal trattamento, ulteriormente incrementata dal PJ34, sia in cellule proficienti che deficienti per PARP-1. Infine, il PJ34 è in grado di aumentare l'apoptosi indotta dal TPT, evidenziato dalla proteolisi di PARP-1 e dalla espressione di BAX e della forma attiva della caspasi 3.

La caratterizzazione della segnalazione del danno indotto dal TPT può essere utile per mettere a punto strategie che superino la chemioresistenza acquisita in seguito al trattamento con gli inibitori di TOP1.

INDEX

LIST OF TABLES AND FIGURES

1. INTRODUCTION

1.1 Poly(ADP-ribose) polymerase (PARP) and Topoisomerse 1 (TOP1) role on DNA damage repair

DNA damage signaling is crucial for the maintenance of genome integrity. In higher eukaryotes a NAD^+-dependent signal transduction mechanism is evolved to protect cells against the genome destabilizing effects of DNA strand breaks.

The mechanism involves two nuclear enzymes, poly(ADP-ribose) polymerase-1 and -2 (PARP-1 and PARP-2), that participate to poly(ADP-ribosyl)ation reaction, a post-translational modification process which plays a critical role in different cellular functions such as DNA damage detection and repair, transcriptional regulation, chromatin modification, and cell death. PARP-1 and -2 bind to DNA strand breaks and form a catalytically active dimer; nicked DNA is stabilized in a V-shaped conformation. Activated PARPs cleave β-NAD^+ in nicotinamide and ADP-ribose to link long and branched (ADP-ribose) polymers (PAR) to glutamic acid residues within the primary sequence of PARP-1 and PARP-2 (automodification) and to other nuclear proteins (heteromodification) like histones, repair proteins, DNA Topoisomerase 1, p53.

ADP-ribose units are linked by α(1''-2') ribosyl-ribose glycosidic bonds in the linear portions of the polymer or by α(1'''-2'') ribosyl-ribose glycosidic linkages at the branching points; their number ranges from a few to over 200 and branching frequency is estimated to be 2%-3% (**Figure 1**).

In DNA-damaged cells, increased poly(ADP-ribose) synthesis due

to PARP-1 and -2 activation is paralleled by an accelerated catabolism that reduces polymer half life from several hours to a few seconds. Poly(ADP-ribose) glycohydrolase (PARG) is responsible for the specific degradation of polymers to monomeric ADP-ribose units and ADP-ribosyl protein lyase cleaves the link between the first ADP-ribose and modified aminoacids *(Malanga et al, 2005)*.

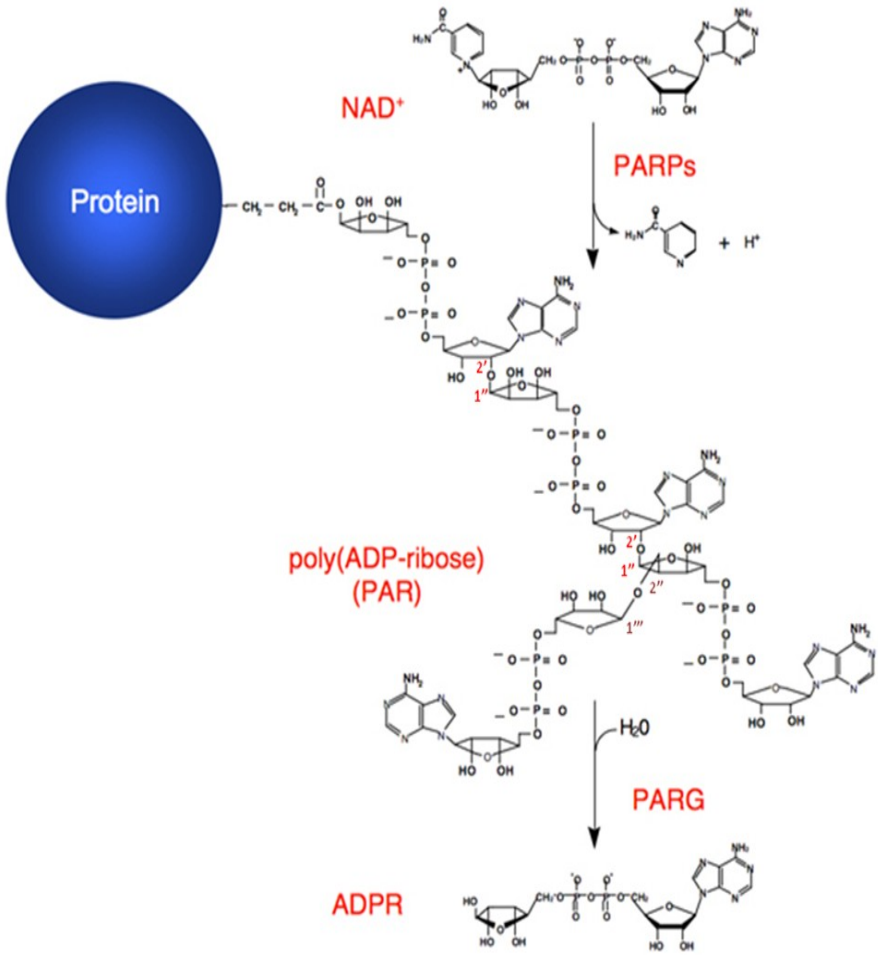

Figure 1. The poly(ADP-ribosyl)ation reaction.

PARP-1 and PARP-2 are members of a large family of enzymes with homologous catalytic domain but with otherwise distinct structures, functions and localizations.

PARP-1 is a 113 kDa nuclear protein comprised of three functional domains:

- the N-terminal DNA-binding domain (DBD) contains the nuclear localization signal (NLS) and two zinc fingers that are important for the binding of PARP-1 to single-strand breaks (SSBs) and double strand breaks (DSBs). A third zinc finger was found to be dispensable for DNA binding and is important for coupling damage-induced changes in the DBD to alterations in catalytic domain;
- in the central automodification domain, specific glutamate and lysine residues serve as PAR acceptors. This domain also comprises a BRCA1 carboxy-terminal (BRCT) repeat motif, a protein-protein interaction domain that is found in other components of the DNA damage response pathway;
- the C-terminal catalytic domain transfers ADP-ribose subunits from β-NAD^+ to protein acceptors.

Some of these recruited proteins bind covalently to polymers, whereas others are indirectly recruited because they contain a PAR-binding consensus sequence. At the same time, the formation of PAR reduces the affinity of PARP-1 and histones for DNA, a mechanism for removing PARP-1 from damaged sites and for the local modulation of chromatin compaction. The removal of PARP-1 provides access for repair proteins, but the enzyme remains in the vicinity of the breaks, recruiting other selected proteins into multiprotein complexes to accelerate DNA damage repair *(Rouleau et al; 2010)*. In contrast, when DNA damage exceeds cell

repair capacity, PARP-1 undergoes cleavage by caspases (3 and 7) into two fragments of 89 kDa and of 24 kDa, thereby avoiding futile cycling of PAR that would otherwise deplete the cell of β-NAD^+ required for the onset of apoptosis *(Scovassi et al; 1999)*.

PARP-2 is a 62 kDa nuclear protein, also able to catalyze DNA damage-dependent automodification and can homo- or hetero-dimerize with PARP-1 (**Figure 2**). Although PARP-2 accounts for only 10-15% of the cellular poly(ADP-ribosyl)ation capacity under genotoxic stress, it can partially compensate for PARP-1 loss in knock-out mice *(Amè et al; 1999)*.

The N-terminal domain of PARP-2 contains NLS, the nucleolar localization signal (NoLS) and a highly basic DBD, that is structurally different from that of PARP-1, probably reflecting differences in the DNA structures recognized by each enzyme (**Figure 2**).

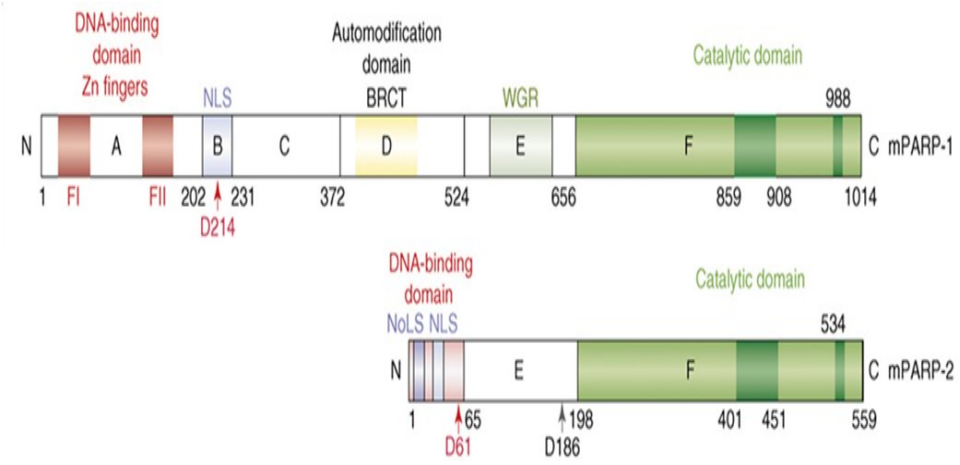

Figure 2. Structure of PARP-1 and PARP-2.

PARP-1 and -2 catalytic domains exhibit 69% similarity; in particular, PARP-2 contains an additional three aminoacid insertion that could reflect specificities in the substrates ADP-ribosylated by this enzyme *(Yelamos et al; 2008)*.

PARP-1 and PARP-2 play a dual role as damage sensors and signal transducers to down-stream effectors (**Figure 3**).

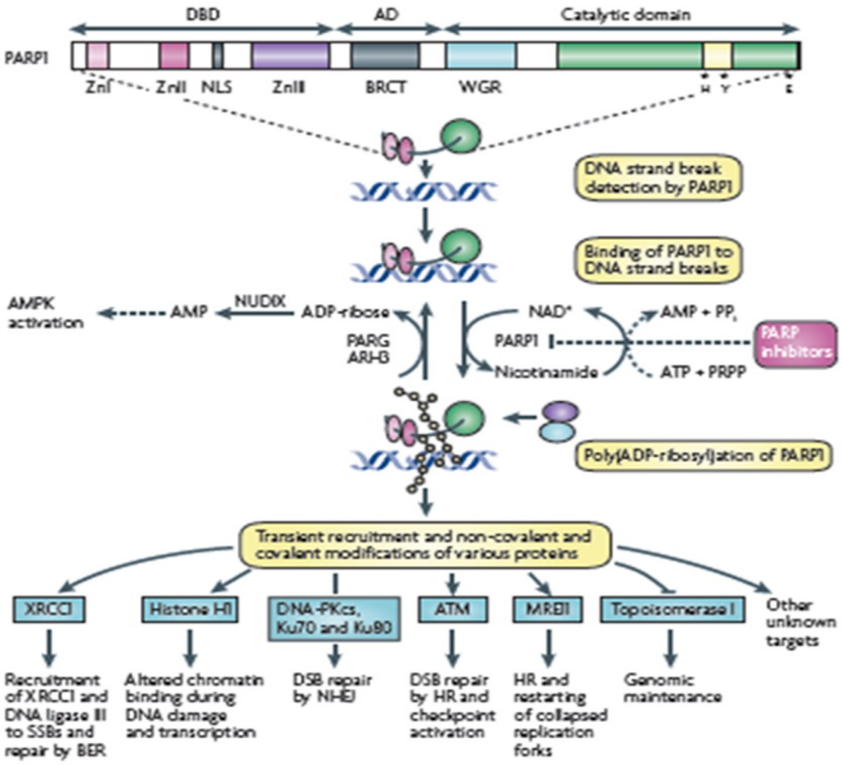

Figure 3. PARP-dependent signaling of DNA strand breaks.

Both proteins share several common nuclear binding partners and have been described as contributors to base excision repair (BER).

In fact, like PARP-1, PARP-2 interacts with X-ray repair cross-

complementing 1 (XRCC1), DNA polymerase β and DNA ligase III, which are involved in BER *(Schreiber et al; 2002)*. However, PARP-1 and -2 were shown to accumulate with different kinetics at laser-induced SSBs: whereas PARP-1 accumulates fast and transiently, PARP-2 shows a delayed and persistent accumulation at repair sites *(Mortusewicz et al; 2007)*.

As mentioned above, PARP-1 binds SSBs while PARP-2 has a higher affinity for gaps and flaps, structures that correspond to more advanced repair intermediates. Taken together, these evidences favour an implication of PARP-2 at later steps of the repair process.

PARP-1 is also involved in DSBs repair process.

Eukaryotes have two pathways for repairing DSBs: homologous recombination (HR) and non homologous end joining (NHEJ). The relative contribution of these two DSBs repair pathways seems to differ depending on the cell cycle phase: HR acts mainly in the S and G2 phases and NHEJ mostly in the G1 phase *(Khanna et al; 2001)*.

In regard HR, a functional and physical interaction between ataxia telangiectasia mutated (ATM) and PARP-1 has been described *(Haince et al; 2007)*; recently, it has been also shown that PARP-1 is able to accumulate at a locally induced DSBs and is required for the accumulation of other DSBs sensors, such as meiotic recombination 11 (MRE11) and Nijmengen breakage syndrome 1 (NBS1) proteins *(Haince et al; 2008)*. Indeed, PARP-1 is reported to interact with and poly(ADP-ribosyl)ate the DNA-PK subunit Ku, an important factor of the alternative pathway NHEJ *(Wang et al; 2006)*.

The role of PARP-2 in DSBs repair still remains to be clarified: it has been observed an interaction between PARP-2 and Ku. An early

embryonic lethality of PARP-2$^{-/-}$ ATM$^{-/-}$ mice is a consequence of the inefficient BER, leading to conversion of unrepaired SSBs to DSBs during replication *(Huber et al; 2004)*.

PARP-1 also affects DSBs repair as indicated by the increased sensitivity of PARP-1-deficient cells to DSB-inducing agents, especially to TOP1 inhibitors.

DNA Topoisomerase 1 (TOP1) is a ubiquitous enzyme that plays multiple functions at the crossroads between replication, transcription and mRNA maturation. TOP1 relaxes DNA supercoiling generated by transcription, replication and chromatin remodeling.

The catalytic cycle of TOP1 starts with the formation of a DNA single-strand break after which it covalently binds to the 3'-end of the DNA phosphodiester backbone, forming TOP1-DNA *cleavable complex* (**Figure 4**). These complexes are reversible intermediates catalyzing the religation reaction of the enzyme.

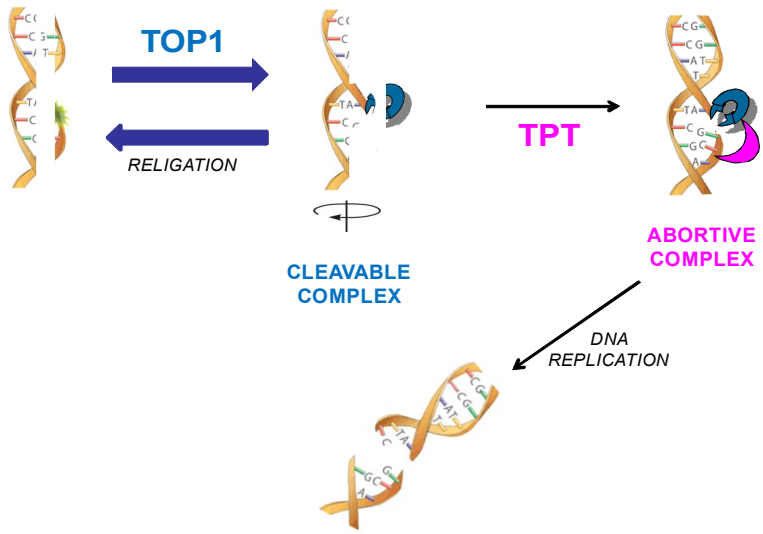

Figure 4. TOP1 catalitic cycle.

Camptothecin (CPT), the prototype of TOP1 inhibitors, and its derivatives such as the clinically relevant drug Topotecan stabilize the cleavable complex in the *abortive complex*, and thus prevents religation step of the enzyme catalytic cycle, generating an accumulation of SSBs. The cytotoxic mechanism of camptothecins is largely S-phase dependent, indicating that is triggered by a collision between replication fork and the abortive complex. This may result in blockage of fork movement, and finally, the formation of DNA DSBs *(Tomicic et al; 2005)*.

The camptothecin derivative Topotecan (TPT) is approved for the treatment of ovarian cancer, non small-cell lung cancer and under clinical investigation for a number of advanced solid tumors and haematological malignancies *(Pommier et al; 2006)*.

For the reason that HR is S phase-dependent, TOP1 poisons-induced replication-dependent DSBs are usually repaired by the HR pathway.

It is known that PARP inhibitors increase the cytotoxic effects of TPT. Furthermore, the molecular mechanism underlying tumor chemosensitization to TOP1 poisons by PARP inhibitors has been in part clarified by recent findings showing that PARP-1 and -2, in their automodified form, counteract camptothecin-action facilitating resealing of DNA strand breaks. This occurs trough non-covalent yet specific interaction of PAR with particular TOP1 sites which results in inhibition of DNA cleavage and stimulation of the religation reaction *(Malanga et al; 2004)*.

The potential of PARP inhibitors to increase the efficacy of chemotherapy has led to the development of a wide range of specific inhibitors – quinazolinone derivatives – like NU1025 and PJ34, which

display increased potency compared to the prototype 3-aminobenzamide (3-ABA) *(Sandhu et al; 2010)*.

In this regard, it has been previously demonstrated a TPT-dependent PARP-1 activation in glioblastoma cells, while co-treatment with the PARP inhibitor NU1025 increased a TPT-dependent p53 up-regulation *(Cimmino et al; 2007)*. Indeed, PARP inhibitors enhance the action of several SSBs-inducing agents, like alkylating agents (i.e. temozolomide) in tumor cell lines and in human tumors. This approach indicates a pairing PARP inhibitors with DNA-damaging therapy to achieve chemosensitization (*Rouleau et al; 2010*).

It has been reported that BRCA1/2 mutated breast carcinoma cells lost their ability to repair DNA breaks after PARP inhibition, which can result in cell cycle arrest and apoptosis, considering that BRCA proteins are critical for the HR pathway *(Bryant et al; 2005)*. This specific killing of tumor cells led to PARP inhibitors entering clinical trials of repair-deficient tumors.

Furthermore, a factor supposed to involved in determining the sensitivity of cells to TOP1 inhibitor is p53. However, for breast cancer cells the p53 status is not found to be predictive for sensitivity to camptothecins *(Davis et al; 1998)*.

1.2 Aim of the work

From the mean of such evidences, we have investigated the role of PARP-1 and PARP-2 in the DNA damage response to TOP1 inhibitor, TPT, in human BRCA1/2$^{+/+}$ and p53$^{+/+}$ breast (MCF7) and cervix (HeLa) carcinoma cells treated with TPT, administered as single agent or in

combination with a PARP inhibitor, PJ34. Furthermore, TPT-sensitivity of HeLa cells in which PARP-1 has been knocked down by RNA interference, has been compared to that of HeLa cells with PJ34.

2. MATERIALS AND METHODS

2.1 Drugs, antibodies and chemicals

TPT and CPT were from *Glaxo Smith-Kline*, PJ34 [N-(6-oxo-5,6,-dihydrophenanthridin-2-yl)-(N,Ndimethylamino)Acetamide] and 3-ABA were from *Alexis Biochemicals*. The cocktail of protease inhibitors was from *ROCHE-Diagnostic*.

Nicotinamide adenine [adenylate-^{32}P] dinucleotide – [^{32}P]-NAD^{+} (1,000 Ci/mmole, 10 mCi/ml) was supplied by *GE Healthcare*.

Propidium iodide (PI) and RNAse were from *Sigma-Aldrich*.

PVDF (poly-vinylidene-fluoride) membrane was from *MILLIPORE S.p.A.* Anti-PARP-1 mouse monoclonal (F1-23) and anti-PARP-2 rabbit polyclonal (Yuc) antibodies were from *Alexis Biochemicals*, anti-DNA Topoisomerase 1 human rabbit polyclonal antibody (Scl-70) from *Topogen* and anti-γH2AX rabbit polyclonal antibody (ser139, 2577) from *Cell Signaling*. Anti-p53 (DO-1), anti-p21 (C-19), anti-Bax (P-19), anti-AIF (E-1), anti-GAPDH (H-2) mouse monoclonal antibodies and anti-Caspase 3 rabbit polyclonal antibody (H-277) were from *Santa-Cruz Biotecnology*. Anti-actin (A2066) rabbit polyclonal antibody and goat anti-mouse and goat anti-rabbit IgG HRP-conjugated antibodies were from *Sigma-Aldrich*.

All other chemicals were of highest quality commercially avaible.

2.2 Cell cultures

Cervix (HeLa) and breast (MCF7) carcinoma cells were maintained in Dulbecco's modified Eagle's medium (DMEM) containing 10% (v/v) heat-inactivated foetal bovine serum (FBS), 100 U/ml penicillin, 100 g/ml

streptomycin, 5 mM L-glutamine and incubated at 37°C in a humidified atmosphere, *plus* 5% CO_2.

Stably PARP-1 silenced HeLa cells (hereafter referred to as $HeLa^{SiP-1}$) or trasfected with pBabe vector carrying the puromycin resistance gene (hereafter referred to as $HeLa^{Babe}$) were obtained as previously described (*Tentori et al; 2010*).

2.3 Cell growth inhibition

MCF7 and HeLa cells were seeded at $1x10^6$ cells; after 24 h, cell cultures were treated with graded concentration of TPT and PJ34 (or 3-ABA) and cell growth inhibition was assessed at different time points (24, 48, 72 h) using trypan blue staining. All the experiments were performed in triplicate.

2.4 Cytofluorimetric analysis

Control and treated cells were detached by enzymatic treatment (Trypsin/EDTA 0.02%), washed in PBS w/o Ca^{2+}/Mg^{2+} pooled with floating cells and recovered by centrifugation at 1,200 rpm for 15 min at 4°C. Cells were fixed in 70% ethanol and stored at -20°C until analysis. After washing in PBS w/o Ca^{2+}/Mg^{2+}, cells were stained in 2 ml of propidium iodide (PI) staining solution [50 μg/ml of PI, 1 mg/ml of RNAse A, 1% Triton X-100 in PBS w/o Ca^{2+}/Mg^{2+}, pH 7.4] overnight at 4°C and DNA flow cytometry was performed in duplicate by a FACScan flow cytometer (*Becton Dickinson Franklin Lakes*) coupled with a CICERO work station (*Cytomation*). Cell cycle analysis was performed by the ModFit LT software (*Verity Software House Inc. Topsham*). FL2

area versus FL2 *width* gating was done to exclude doublets from G2/M region. For each sample 15,000 events were stored in list mode file.

2.5 Alkaline Comet Assay

Cells were suspended in PBS at a density of 10^4 cells/ml and mixed with an equal volume of fresh low-melting agarose (LMA, 1% in PBS); 80 μl of agarose cell suspension was spread on normal-melting agarose (NMA, 1% in PBS) slides and covered with a cover-slip. Two slides were prepared *per* sample. After gelling for 5 min on an ice bed, the cover-slip was gently removed and another layer was added, cover-slipped and allowed to solidify for 5 min on ice before gently removing the cover-slip. The slides were then immersed in a freshly prepared ice-cold lysis solution (2.5 M NaCl, 0.1 M Na_2EDTA, 0.01 M Tris, 1% Triton X-100, 10% DMSO, pH 10) for 1 h. The slides were drained and placed in a horizontal electrophoresis tank filled with freshly prepared alkaline buffer (0.3 M NaOH, 1 mM Na_2EDTA, pH 13) and electrophoresis carried out for 20 min at 300 mA. Finally, the slides were gently washed twice in a neutralization buffer (Tris-HCl 0.4 M, pH 7.5) for 5 minutes to remove alkali and detergent, and stained with 50 μl/ml DAPI (3h). Images of a minimum of hundred cells from each sample were analysed on a fluorescence microscope (*Nikon Instruments S.p.A.*); overlapping figures were avoided from each slide. Quantitative assessment of DNA damage was performed using Comet Score 1.5 Image Analysis (*TriTek Corporation*) software, which computes the integrated intensity profile for each cell. DNA damage was measured as olive tail moment value [(Tail mean - Head mean) x % DNA in tail/100]. The results were

analysed by Student's *t*-test and were considered statistically significant at $P<0.008$.

2.6 Analysis of [^{32}P]-PAR synthesis

Following treatment with 10 μM +/- 5 μM PJ34 of intact cells ($5x10^6$ cells/plate), [^{32}P]-PAR synthesis was determined by substituting the culture medium with 1 ml of 56 mM HEPES buffer pH 7.5, containing 28 mM KCl, 28 mM NaCl, 2 mM $MgCl_2$, 0.01% digitonin, 0.1 mM PMSF, 1:25 dilution of a cocktail of protease inhibitors, 0.125 μM [^{32}P]-NAD^+ (1,000 Ci/mmole). After incubation at 37°C for 30 min, cells were scraped off the plates, transferred to eppendorf tubes and mixed with TCA at 20% (w/v) final concentration. After 15 min standing on ice, samples were collected by centrifugation at 1,200 rpm for 15 min, washed twice with 5% TCA and three times with ethanol. [^{32}P]-PAR incorporated in the TCA-insoluble fraction was measured by Cerenkov counting using a LS8100 liquid scintillation spectrometer (Beckman Coulter S.p.A.). Finally, TCA protein pellets were resuspended in Laemmli buffer; proteins were separated by 5-15% SDS-PAGE and after electroblotting on PVDF membrane, [^{32}P]-PAR acceptors were visualized by autoradiography. Immunodetection of specific proteins was accomplished on the same blots after autoradiography.

PJ34 efficacy as PARP inhibitor was determined in an *in vitro* enzymatic activity assay using permeabilized cells: cell pellets were resuspended in 40 mM Tris-HCl pH 7.8, 0.6 mM EDTA, 30 mM $MgCl_2$, 0.05% Triton X-100, 1mM β-mercaptoethanol, 20% glycerol, 1 mM PMSF and 1:25 dilution of the cocktail of protease. To maximally

stimulate PAR synthesis, DNA strand breaks were induced by sonication for 30 sec at medium intensity; finally, samples were incubated at 30°C for 1 h with 5μCi/ml [^{32}P]-NAD$^+$ and 50 μM unlabeled β-NAD$^+$, in the presence or absence of 5 μM PJ34. Reactions were stopped by TCA addition (20% final concentration) and the samples were processed and analysed as described above.

2.7 Isolation of nuclear and post-nuclear fractions

To isolate sub-cellular fractions, cells were suspended in a buffer containing 30 mM Tris-HCl pH 7.5, 1.5 mM $MgCl_2$, 10 mM KCl, 1% Triton X-100, 20% glycerol, 2 mM PMSF and the protease inhibitors cocktail solution. After 30 min of incubation on ice, cellular suspensions were centrifuged at 960 x g for 90 sec at 4°C and the nuclear fractions recovered in the pellet. The supernatant represents the post-nuclear fraction.

Nuclear fractions were resuspended in 20 mM HEPES pH 7.9, containing 20 mM KCl, 0.2 mM EDTA, 1.5 mM $MgCl_2$, 25% glycerol and 0.2 mM PMSF. Protein concentration was determined using the Bradford protein assay reagent (*BIO-RAD*) with bovine serum albumin (BSA) as a standard.

2.8 Autoradiographic and immunological analyses

Aliquots of 120 μg of cellular proteins were separated by SDS-PAGE (5-15% gradient gels) and transferred onto a PVDF membrane using an electroblotting apparatus (*BIO-RAD*). The membrane was subjected to autoradiographic analysis by the PhosphorImager (*BIO-RAD*)

and/or to immunodetection after blocking with 3% BSA in TBST 1 h, with anti-PARP-1 (diluted 1:5,000), anti-PARP-2 (diluted 1:5,000), anti-TOP1 (diluted 1:2,500), anti-p53 (diluted 1:5,000), anti-p21 (diluted 1:1,000), anti-Bax (diluted 1:500), anti-AIF (diluted 1:500), anti-Caspase 3 (diluted 1:500), anti-GAPDH (diluted 1:5,000), anti-γH2AX (diluted 1:1,000) or anti-actin (diluted 1:1,000).

As secondary antibodies goat-anti-mouse or goat-anti-rabbit IgG HRP-conjugate (diluted 1:10,000-1:20,000) in 3% (w/v) non-fat milk in TBST were used. Peroxidase activity was detected using the ECL Advance Western Blotting Kit (*GE Healthcare*) and quantified using the Immuno-Star Chemiluminescent detection system GS710 (*BIO-RAD*) and the Arbitrary Densitometric Units normalized on those of the GAPDH loading control.

3. RESULTS

3.1 Effect of PARP inhibitors on TPT-induced growth inhibition and cell cycle distribution in human carcinoma cells

In preliminary experiments, we evaluated a dose-response of MCF7 cells to TPT, alone or in combination with 5 μM PJ34 at 24-48 h treatment. As shown in **Figure 5**, TPT alone caused a strong cytotoxic effect at 24 h, starting from 5 μM concentration (60% cell growth inhibition), while the same amount of PJ34 and 1 μM TPT slightly affected cell growth inhibition (18%). Therefore, in this condition it was difficult to evaluate additive/synergic effect of combined treatment.

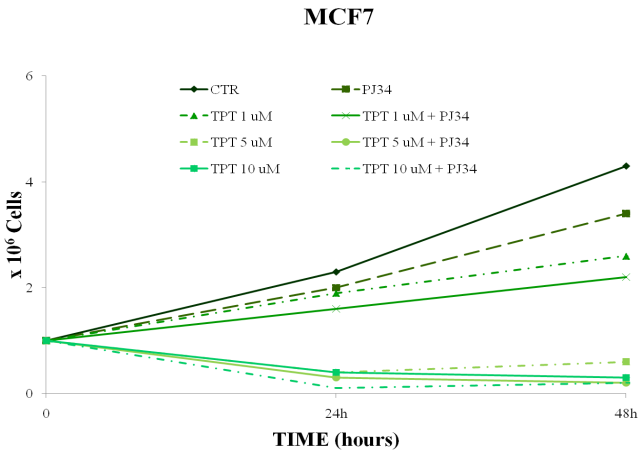

Figure 5. Dose-dependece response of MCF7 cells to TPT in presence or absence PJ34.
MCF7 cells were treated for 24 - 48 h with TPT (1 – 5 – 10 μM) in combination or not with PJ34 (5 μM). The results are the mean of three different experiments giving similar results.

For further experiments we set up 1 h treatment condition with 10 μM TPT followed by different recovery times in the presence or not of

5 μM PJ34. Furthermore, stably PARP-1 silenced HeLa cells (HeLa^{SiP-1}) were also compared to PARP-1 proficient HeLa cells (HeLa^{Babe}).

Both HeLa^{Babe} and MCF7 cells showed till 72 h after treatment mainly a cytostatic effect (**Figure 6**), whereas PARP-1 silencing rendered HeLa^{SiP-1} cells more sensitive to the drug, causing 45% of cells to die (**Figure 7**). The presence of PARP inhibitor during the recovery time seemed to increase TPT-toxicity, also in PARP-1 deficient cells.

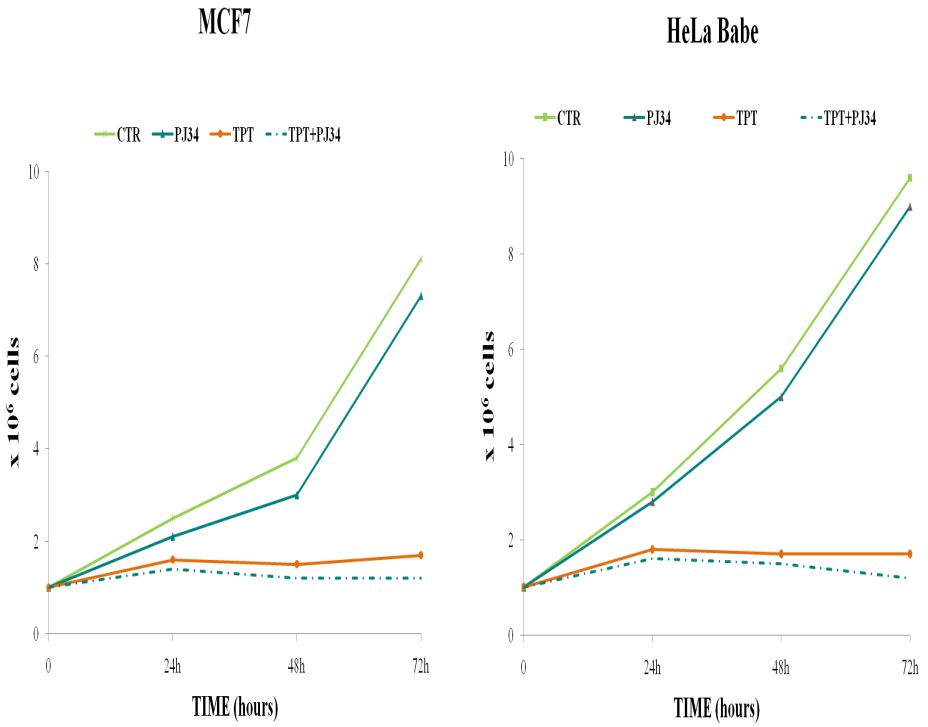

Figure 6. Cell growth inhibition of MCF7 and HeLa^{Babe} cells treated with TPT and PJ34 as single agents or in combination.
The cells were treated for 1 h with 10 μM TPT+/- 5 μM PJ34 and left to recover 24, 48 e 72 h in fresh medium in the presence or not of PARP inhibitor. The results are the mean of three different experiments giving similar results.

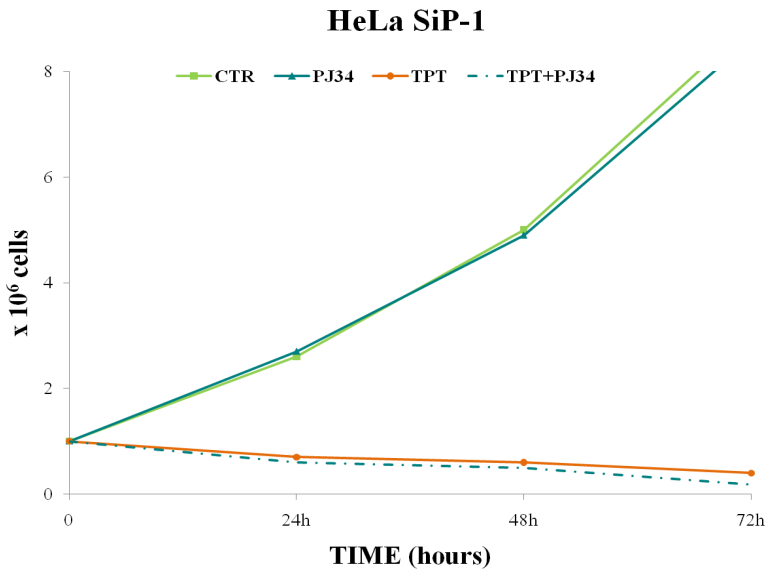

Figure 7. Cell growth inhibition of HeLa^{SiP-1} cells treated with TPT and PJ34 as single agents or in combination.
The cells were treated for 1 h with 10 μM TPT+/- 5 μM PJ34 and left to recover 24, 48 e 72 h in fresh medium in the presence or not of PJ34. The results are the mean of three different experiments giving similar results.

Figure 8 shows a comparison of cell growth inhibition determined in MCF7 cells by treatment with TOP1 inhibitors (CPT and TPT) as single agents at the same concentration or in combination with PJ34 or 3-ABA. By the all of the results we observed an additive effect of the PARP inhibitors on the cytostatic effect of TPT. Interestingly, the same increment on cell growth inhibition was observed by a 200 times dose reduction of PJ34 with respect to 3-ABA.

CPT, instead, caused a cytotoxic effect *per se*, even higher than that determined by TPT+PJ34 (or 3-ABA) combination. Therefore, no additive effect was observed by PJ34 and 3-ABA on CPT-action.

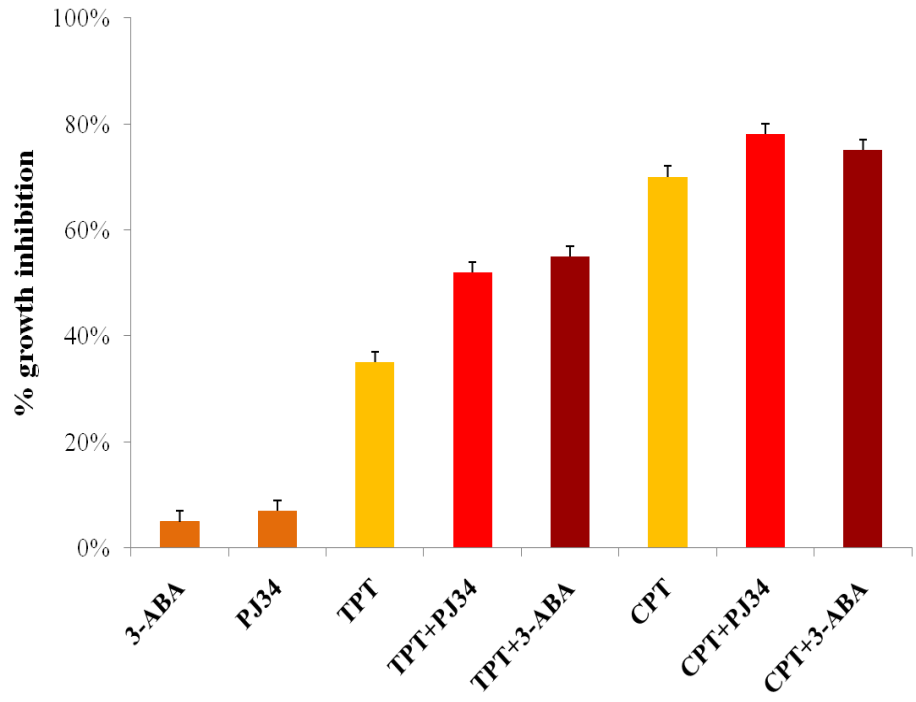

Figure 8. Comparison of TPT and CPT as single agents or combined with PARP inhibitors.
MCF7 cells were treated for 1 h with 10 μM TPT or 10 μM CPT +/- 5μM PJ34 or 1mM 3-ABA and left to recover 24 h in fresh medium in the presence or not of PJ34 or 3-ABA. The results are expressed as percentages of growth inhibition +/- S.E.

To go better inside into the mechanism of enhanced TPT-toxicity as a consequence of alteration of the cellular poly(ADP-ribosyl)ation status, we analysed cell cycle distribution 24 h after 1 h treatment with increasing concentrations of TPT in the presence or not of fixed concentration of 5 μM PJ34.

As shown in **Figure 9A**, in HeLa^{Babe} cells graded concentrations of TPT induced a progressive increase of cell accumulation in the G2/M phase starting from 0.2 μM up to 1.25 μM; higher TPT-doses, instead,

caused the well known TPT-specific S phase arrest. Then, the addition of PJ34 to TPT-concentrations < 1.25 µM significantly increased G2/M cell accumulation, whereas combined with ≥ 1.25 µM TPT concentrations induced S phase block of cells (that would escape TPT-action).

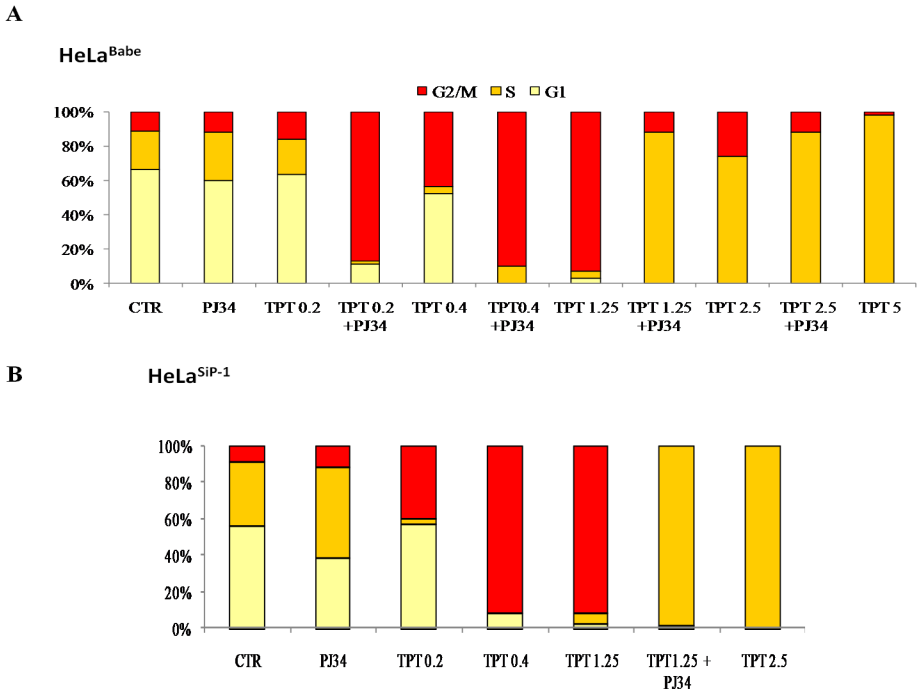

Figure 9. Cell cycle analysis of HeLa cells treated with TPT and PJ34 as single agents or in combination.
Babe and SiP-1 cells were treated for 1 h with TPT (0.2 – 0.4 – 1.25 – 2.5 – 5 µM) +/- PJ34 (5 µM) and left to recover 24 h in fresh medium in the presence or not of PJ34. The results are expressed as percentages of cells in the G1, S and G2/M phase of the cell cycle.

As shown in **Figure 10**, cell cycle distribution was unaffected by treatment of HeLa^{Babe} cells with 5 µM PJ34 and 1 mM 3-ABA used as single agents. Moreover, when combined with 1.25 µM TPT 3-ABA

caused a minor S phase accumulation (27%) compare to PJ34 (78%), confirming the enhanced potency of this later PARP inhibitor.

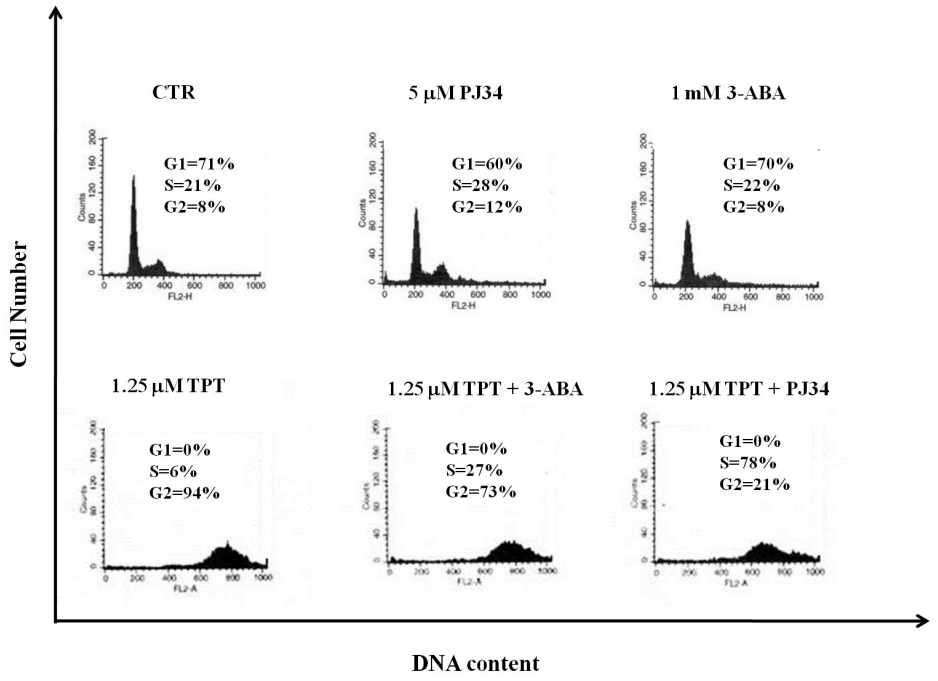

Figure 10. Cell cycle analysis of HeLa^{Babe} cells treated with TPT and PARP inhibitors as single agents or in combination.
Babe cells were treated for 1 h with 1.25 μM TPT +/- 5 μM PJ34 or 1 mM 3-ABA and left to recover 24 h in fresh medium in the presence or not of PJ34 or 3-ABA. Flow cytometric determination of DNA content after PI staining is shown. The percentage of cells in the G1, S and G2/M is indicated.

Accordingly, HeLa^{SiP-1} cells underwent a more pronounced increase of G2/M phase or S phase accumulation, with respect to HeLa^{Babe} cells exposed to the same doses of TPT; interestingly, the combination 1.25 μM TPT and 5 μM PJ34 induced S phase accumulation at higher extent than HeLa^{Babe} (**Figure 9B**).

Cytofluorimetric analysis at longer recovery times (i.e. 72 h after 1

h treatment) revealed that the alteration of the poly(ADP-ribosyl)ation system determined the induction of apoptosis, as indicated by the appearance of a sub-diploid peak. In particular, the lack of PARP-1 appeared to be more effective than PARP activity inhibition as the fraction of apoptotic cells was doubled in HeLa^{SiP-1} treated with 1.25 μM TPT (62%) *versus* HeLa^{Babe} subjected to a combined TPT+PJ34 treatment (38%) (**Figure 11**).

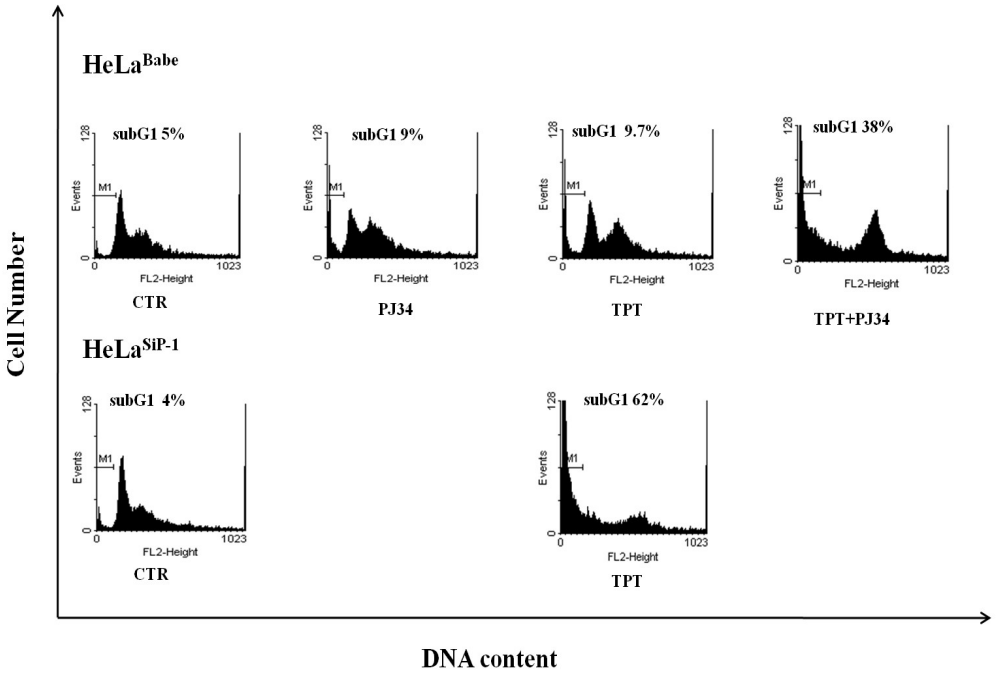

Figure 11. Cell death analysis of HeLa cells subjected to TPT+/-PJ34 treatment.

Babe and SiP-1 cells were treated for 1 h with 1.25 μM TPT +/- 5 μM PJ34 and left to recover 72 h in fresh medium in the presence or not of PJ34. Flow cytometric determination of DNA content after PI staining is shown. The percentage of cells in the sub-diploid (subG1) peak is indicated.

3.2 Analysis of TPT- and/or PJ34-dependent DNA damage in carcinoma cells

By alkaline comet assay, we analysed the level of both DNA SSBs and DSBs arising 24 h after 10 μM TPT +/- 5 PJ34 μM 1 h treatment. **Figure 12A** shows that the olive tail moment value was comparable in all cell lines and further increased in the cells left to recover in the presence of PJ34, either PARP-1 proficient or silenced cells.

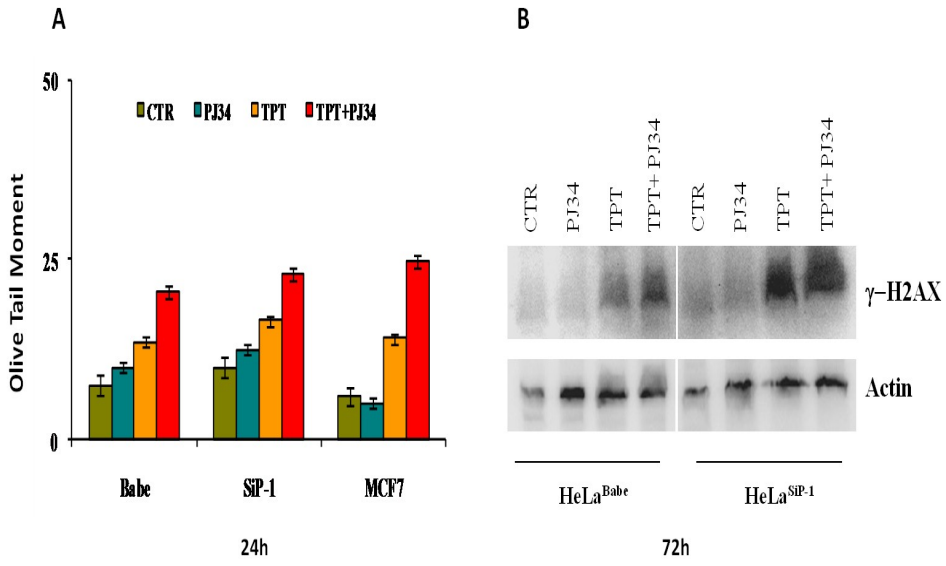

Figure 12. DNA damage in carcinoma cells subjected to TPT+/- PJ34 treatment.

A: Hundred cells 24 h after 1 h treatment with 10 μM TPT +/- 5 μM PJ34 were analysed by alkaline comet assay on a fluorescence microscope and quantitative assessment of DNA damage was performed using Comet Score.

B: Western blot analysis of γH2AX levels in Babe and SiP-1 cell nuclei treated 1 h with 10 μM TPT and allowed to recover in fresh medium in the presence or not of 5 μM PJ34 for 72 h. Actin was used as loading control.

The definition of a DSBs level was obtained by looking at H2AX phosphorylation in isolated nuclei from Babe and SiP-1 cells. **Figure 12B** shows a TPT-dependent increase of γ-H2AX in HeLa cells until 72 h after treatment that was further increased after TPT+PJ34 cotreatment. Interestingly, the further increment determined by PJ34 in PARP-1 silcenced cells was suggestive of the involvement of PARP-2 (or some other PARP).

3.3 Analysis of PAR synthesis in carcinoma cells after treatment with TPT +/- PJ34

First, PJ34 efficacy as PARP inhibitor at 5 μM concentration was assessed by an *in vitro* enzyme activity assay, carried out in sonicated cells incubated with exogenous 50 μM [^{32}P]-NAD$^+$ in the presence or not of PJ34. Sonication was performed to induce DNA strand breaks and thus maximally stimulate endogenous PARP activities.

As shown in **Figure 13A**, a high amount of protein-bound PAR was produced in HeLa^{Babe} cells and such an activity was completely abolished by 5 μM PJ34.

The corresponding immunodetection showed a reduction of PARP-1 native protein in the sample incubated with β-NAD$^+$ alone compared to that incubated with β-NAD$^+$ + PJ34. Such a difference is explained by a band depletion due to the automodification-related electrophoretic mobility shift of a fraction of heavily poly(ADP-ribosylated) PARP-1. After quantification of immunoreactive bands by scanning densitometry and normalization of PARP-1 to GAPDH content, it could be estimated that about 50% of PARP-1 underwent automodification (**Figure 13B**).

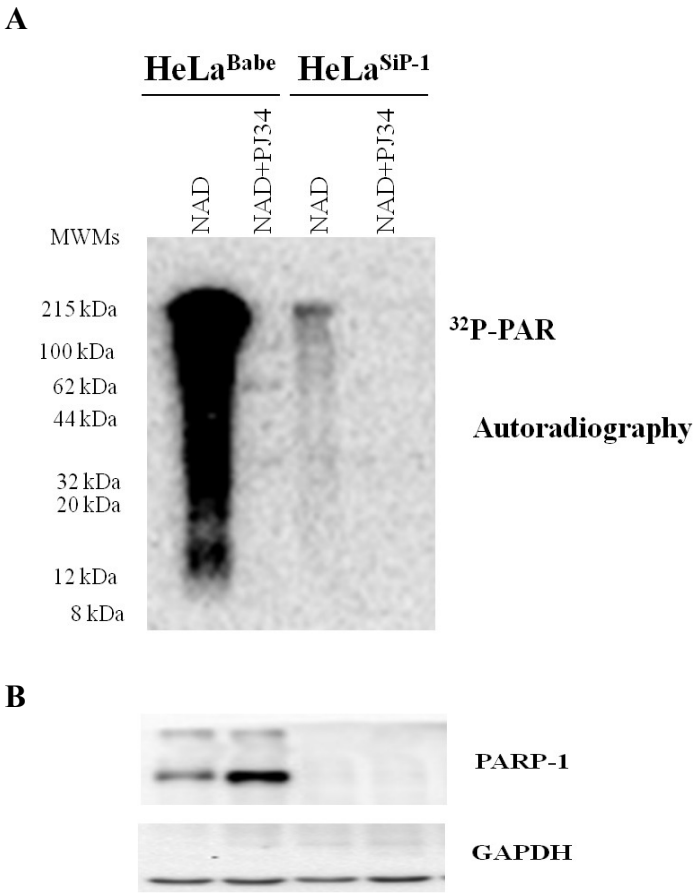

Figure 13. PJ34-dependent inhibition of PAR synthesis in HeLa cells.
Babe and SiP-1 cells were resuspended in permeabilizing buffer, sonicated and incubated with 50 μM [^{32}P]-NAD^{+} +/- 5 μM PJ34, as described in M&M.
A: Autoradiographic analysis of whole cell protein after SDS-PAGE and electroblot on PVDF.
B: Immunodetection of PARP-1 and GAPDH on the blot shown in A.

The same kind of analysis carried out on HeLa^{SiP-1} cells revealed a strongly reduced ADP-ribosylation capacity of these cells: in fact, in the autoradiography only a light smear at top of the gel was visualized (**Figure 13A**) and by western blotting no PARP-1 was detected (**Figure 13B**), as a consequence of silencing. This modest ADP-ribosylation activity detected (about 18%), may be due to PARP-2 (or other PARPs) or to a residual PARP-1 protein: anyway it was also inhibited by PJ34.

Then, we used a different experimental setting to determine whether or not TPT could induce PARPs activation in growing cells. To this purpose, the MCF7 cells were first exposed to the drugs and then PAR synthesis was measured *in situ* by incubation of permeabilized cells with 0.125 μM [^{32}P]-NAD^{+}.

The autoradiography showed a main signal up to PARP-1 molecular weight (113 kDa), indicating a TPT-dependent PARP-1 automodification, that appeared already after 1 h treatment and was sustained for 24 h recovery time (**Figure 14**).

A minor autoradiographic signal in the 90-50 kDa MWs range could be attributed to a modified PARP-2 (62 kDa), on the basis of a modification-related electrophoretic mobility shift.

The radioactive signals were significantly reduced in cells co-treated with TPT+PJ34, accordingly with a 75% decrease of the [^{32}P]-PAR incorporated in the TCA-insoluble fraction with respect to cells treated with TPT alone, measured by the use of the liquid scintillation spectrometer.

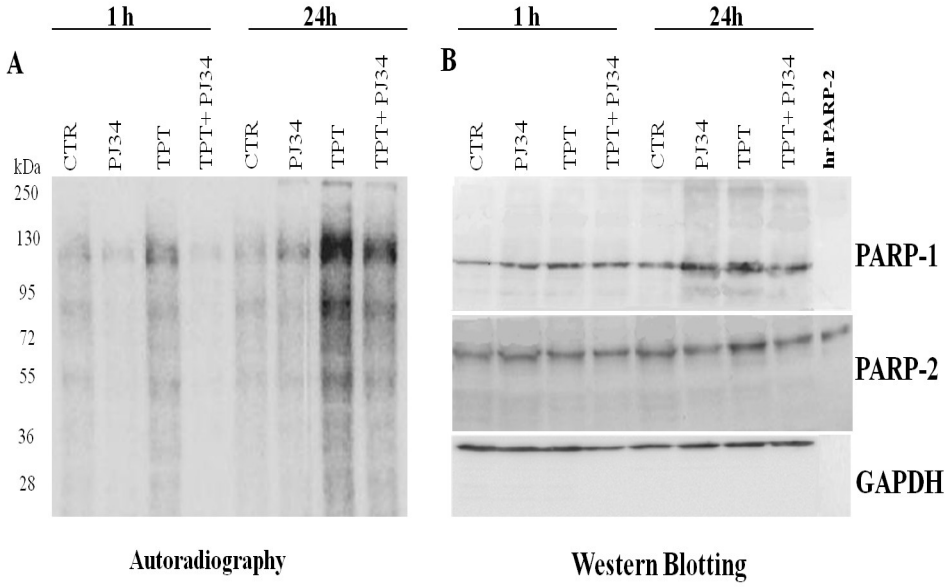

Figure 14. TPT-dependent PARPs activation in MCF7 cells.
Following 1h treatment with 10 μM TPT +/- 5 μM PJ34 and recovery for 24 h in fresh medium in the presence or not of PJ34, MCF7 cells were incubated with 0.125 μM [^{32}P]-NAD^{+}, as described in M&M.
A: Autoradiographic analysis of whole cell protein after SDS-PAGE and electroblot on PVDF.
B: Immunodetection of PARP-1, PARP-2 and GAPDH on the blot shown in A. Fifty ng of human recombinant PARP-2 (hrPARP-2) was also loaded as a standard.

3.4 Immunological analysis of different protein level in TPT +/- PJ34 treated carcinoma cells

By western blotting, we looked at TPT-dependent changes in the endogenous levels of several proteins in HeLa and MCF7 cells at different times (24, 48 and 72 h) after 1 h treatment with 10 μM TPT +/- PJ34.

Figure 15 shows that the amount of soluble/active TOP1 was lowered till 72 h recovery times, as a consequence of the treatments. Conversely, it was observed an up-regulation of p53 levels in the same time frame and the concomitant p53-dependent p21 induction, starting from 24 h after TPT-treatment.

The same results were evident in HeLa cells (**Figure 16**): in particular, the TPT-dependent p53 up-regulation was even higher in $HeLa^{SiP-1}$ cells and further increased by TPT and PJ34 co-treatment, with respect to $HeLa^{Babe}$ cells.

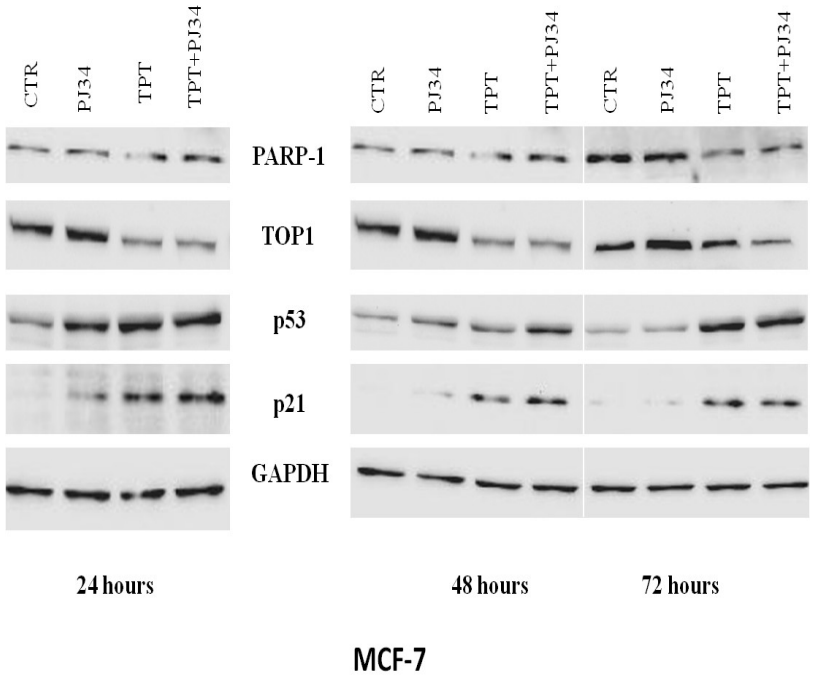

Figure 15. Western blot analysis of PARP-1, TOP1, p53 and p21 in MCF7 cells.

MCF7 cells were treated with 10 μM TPT+/- 5 μM PJ34 for 1 h and allowed to recover in fresh medium in the presence or not of PJ34 for the indicated times. GAPDH was used as loading control.

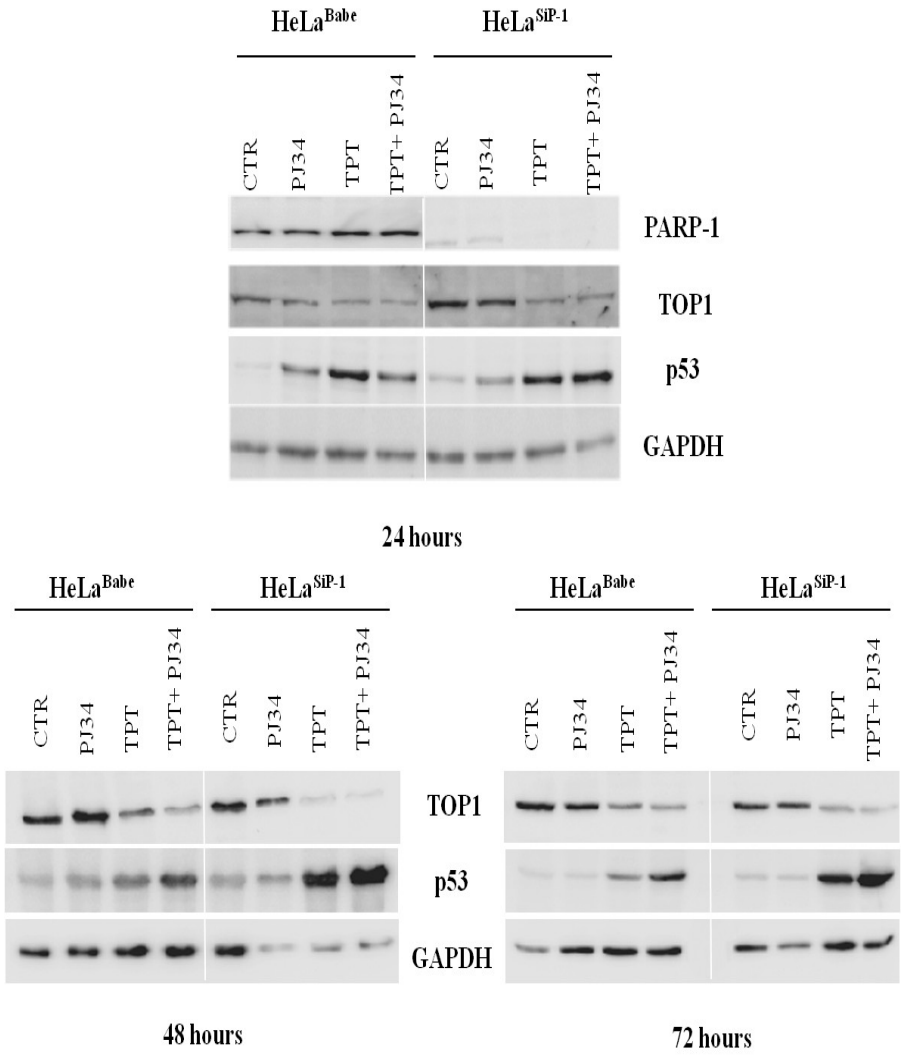

Figure 16. Western blot analysis of PARP-1, TOP1 and p53 in HeLa cells.

Babe and SiP-1 cells were treated with 10 μM TPT+/- 5 μM PJ34 for 1 h and allowed to recover in fresh medium in the presence or not of PJ34 for the indicated times. GAPDH was used as loading control.

Indeed, we also confirmed the p53 activation by looking to its nuclear stabilization in HeLa cells. **Figure 17** shows a TPT-dependent increase of nuclear p53-localization arising 24 h after treatment, that was even higher as a consequence of PJ34 addition.

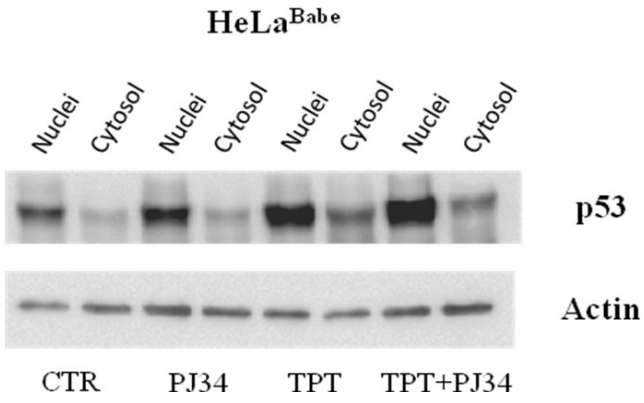

Figure 17. p53 nuclear stabilization in HeLa cells.
Western blot analysis of p53 levels in Babe cell nuclei treated 1 h with 10 μM TPT+/- 5 μM PJ34 and allowed to recover in fresh medium in the presence or not of PJ34 for 24 h. Actin was used as loading control.

By densitometric scanning of immunoreactive bands of **Figure 16**, we quantified the changes in p53 levels at different times after single and combined treatments.

As shown in **Figure 18**, 72 h after 1 h treatment, we calculated a 10 fold increase of p53 levels in HeLa^{SiP-1} cells compared with 2.25 fold in HeLa^{Babe} cells treated with TPT alone; these values were increased to 13 fold and 4.5 fold in SiP-1 and Babe respectively, by the presence of PJ34 during the recovery time.

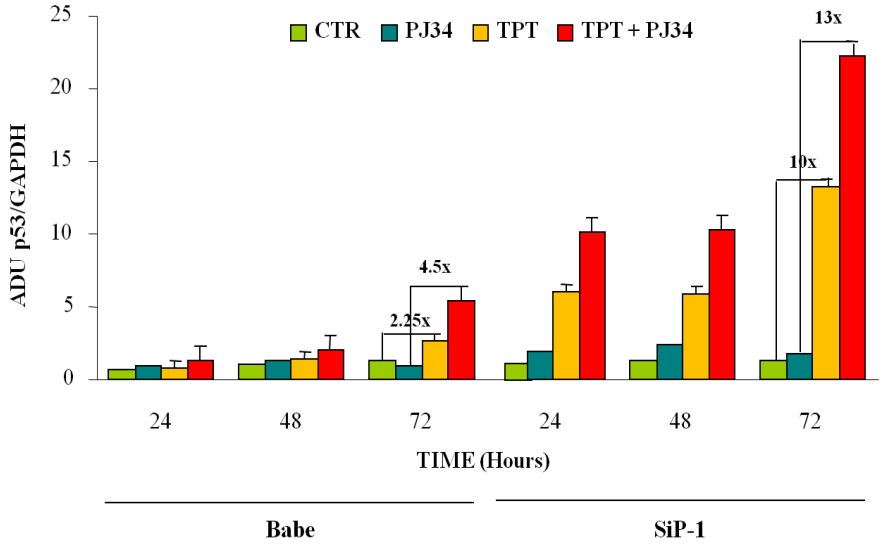

Figure 18. Densitometric analysis of p53 levels in HeLa cells.
After immunodetection on western blot, band intensities were quantified by scanning densitometry. Data, expressed as Arbitrary Densitometric Units (ADU), were normalized to the internal control GAPDH.

Finally, at longer recovery times we analysed the expression of apoptotic markers.

As shown in **Figure 19A**, in HeLa^{Babe} cells it was evident the caspase-dependent PARP-1 cleavage. Instead, in MCF7 cells the PARP-1 apoptotic fragment was hardly detectable, but we observed the p53-dependent BAX expression. Interestingly, we found that PJ34 was able to enhance both such apoptotic signals.

Moreover, we looked for other apoptotic markers in isolated nuclei of HeLa^{SiP-1} cells.

In **Figure 19B**, it couldn't observed any nuclear traslocation of AIF (Apoptosis-Inducing Factor) in treated cells, but it was evident the active form of caspase 3 in nuclei from TPT-treated cells, incremented by TPT+PJ34 combined treatment.

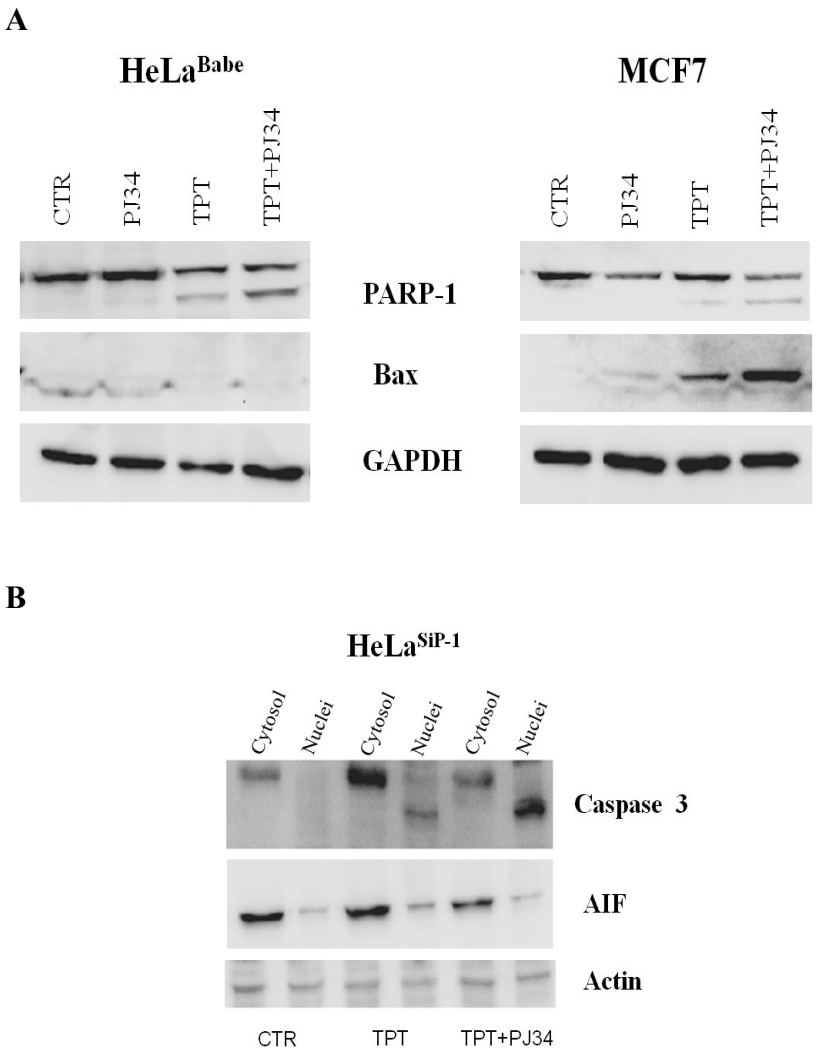

Figure 19. Apoptotic markers in carcinoma cells.
Cells were treated with 10 μM TPT+/- 5 μM PJ34 for 1 h and allowed to recover in fresh medium in the presence or not of PJ34 for 72 h.
A: Western blot analysis of PARP-1 and Bax in HeLa^{Babe} and MCF7 cells. GAPDH was used as loading control.
B: Western blot analysis of AIF and Caspase 3 in HeLa^{SiP-1} cell nuclei. Actin was used as loading control.

4. DISCUSSION

Clinical investigation of PARP inhibitors follows two distinct approaches: targeting cells that are genetically predisposed (repair-deficient) to die when PARP activity is lost; and combining PARP inhibition with DNA-damaging therapy to derive additional therapeutic benefit from DNA damage. This has led to the development of a multitude of potent PARP inhibitors with various bioavailability and pharmacokinetic characteristic whose efficacy in the treatment of cancer *in vivo* has been evaluated in animal models (*Tentori et al; 2005*).

In our studies, we used the hydrophilic PARP inhibitor PJ34 that has been recently reported to synergize with cisplatin in triple-negative breast cancer (*Hastak et al; 2010*) and colon carcinoma (*Gambi et al; 2008*) cell lines, in combination with the DNA Topoisomerase 1 inhibitor TPT. For our experiments, we performed 1 h treatment up to 10 μM TPT that was already reported to be sufficient for trapping TOP1 in MCF7 cells (*Feeney et al; 2003*). PJ34 was used at 5 μM concentration that was efficient at inhibiting PARP activity, while not being cytotoxic *per se*.We found that TPT toxicity was higher when PAR synthesis was strongly reduced by either PARP-1 silencing ($HeLa^{SiP-1}$ cells) or PJ34 administration (both in HeLa and MCF7 cells), as indicated by cell growth and cell cycle analysis.

In fact, MCF7 and HeLa cells, according with their comparable PARP-$1^{+/+}$, BRCA1/$2^{+/+}$ and $p53^{+/+}$ status showed the same sensitivity to TPT, which determined a cytostatic effect and a cell cycle arrest until 72 h after treatment. However, in combination with PJ34, TPT was cytotoxic even at a very low concentration (1.25 μM). Accordingly, TPT alone was

cytotoxic in HeLa^{SiP-1}. Interestingly, the PARP inhibitor further increased the sensitivity of SiP-1 cells treated with the drug combination, suggesting a PARP-2 involvement in the signaling of TPT-dependent DNA damage. So, TPT-treated cells entered the apoptotic program as a consequence of PARP-1 silencing and/or PARP inhibition.

Consistently with the idea that poly(ADP-ribosyl)ation plays a role in the response to TPT-induced DNA damage, we found increased PAR synthesis following cell exposure to 10 μM TPT. The lack of PAR synthesis, by interfering with the repair of TOP1-induced DNA damage causes DNA strand break accumulation and further delays cell cycle progression.

In particular, we observed distinct cell cycle perturbation effects depending on the concentration of TOP1 poison and on the association with the PARP inhibitor: PJ34 in combination with 0.2 - 0.4 μM TPT caused more cells to be arrested in G2/M phase, while combined with 1.25 μM TPT induced a S phase block, not observed in TPT+3-ABA co-treated cells. Furthermore, the G2/M arrest induced by 0.4 μM TPT in PARP-1 wild type cells was magnified in PARP-1 silenced HeLa cells.

These evidences agree with the concept that after 1 h pulse of TPT not all the cells are prevented from entry in mitosis and the G2 cell lineages could survive TPT-mediated cytotoxicity (*Tuduri et al; 2009*). Therefore, the persistence of cells at the G2/M phase provoked by PARP inhibition and PARP-1 silencing can be seen as a mechanism to overcome cell resistance to camptothecin derivates. Interestingly, in PARP-1 silenced HeLa cells PJ34 increased the TPT-dependent S phase block as further indication of PARP-2 implication.

Indeed, the TPT-dependent DNA damage level was increased by

co-treatment with PJ34 either in PARP-1 proficient and silenced cells 24 h after treatment . In nuclei of such cells, differences in γH2AX levels deriving from TPT+/- PJ34 exposure support the involvement not only for PARP-1 but also for PARP-2 in the signaling of TPT-dependent DSBs repair.

Moreover, we found a sustained PAR synthesis from 1 to 24 h after treatment and most of the newly synthesized polymer was linked to PARP-1 itself. Another PAR acceptor (probably PARP-2) in the lower molecular weight range appeared to be TPT-dependent. Accordingly with the magnified effect of TPT+PJ34 co-treatment in $HeLa^{SiP-1}$, the PARP-2 modification could represent the mechanism of its participation in DSBs signaling and HR repair (*Yelamos at al; 2008*).

PARP activity assays also offered an indication of PJ34 inhibitory efficacy. We already showed that 5 μM PJ34 totally inhibits PARP activity *in vitro*; according with the *in situ* assays we determined approximatively 75% PARP inhibition in permeabilised cells. This could also explain quantitative differences observed in the use of inhibitors compared to PARP-1 silencing. Indeed, our results also confirmed that PJ34, as its prototype 3-ABA, do not discriminate between PARPs enzyme. Then, PARP-1 silenced cells allowed the attribution of a residual PARP activity (12%) to PARP-2.

The last set of results was based on mechanistic investigations addressed to show the long-term response to TPT action: after 1 h pulse TOP1 soluble/active fraction was drastically reduced for at least 3 cell duplication cycle, otherwise p53 levels increased within the same time frame. Such an up-regulation was even higher in cell lacking PARP-1 and further increased by TPT+PJ34 treatment, supporting again the

involvement of PARP-2 in the signaling of TPT-dependent DNA damage. These results are in agreement with those previously reported in the same cells treated with the methylating agent temozolomide in combination with the PARP inhibitor GPI 15427, suggesting the implication of PARP-2 in the repair of another DNA damage-inducing agent (*Tentori et al; 2010*).

We also observed that caspase 3 activation, caspase-dependent PARP-1 proteolysis and p53-dependent BAX expression were sustained by the PARP inhibitor as a result of apoptosis induction.

By the all of such evidences, we envisaged a TPT-dependent DNA damage signaling network, involving PARPs. In fact, the DNA damage arising from the trapping of TOP1 was signaled by PARP-1 and -2 and gathered by effectors like p53/p21. Previous results suggest that p53 causes resistance of cells to TPT exposure (*Tomicic et al; 2003*). Our findings suggest a PARP activation induced by TPT-dependent double strand breaks, while PARP-1 and -2 inhibition switches on p53 pro-apoptotic role.

Indeed, caspase-dependent PARP-1 proteolysis contributes to restoring the apoptotic program in neoplastic cells and has been described in camptothecin-induced apoptosis as an early event that precedes the mitochondrial release of cytocrome c and AIF (*Rodriguez-Hernandez et al; 2006*).

In conclusion, our findings contribute to the understanding the molecular events triggered by TOP1 poisons-dependent genomic damage and the confirming the potential of PARP inhibitors as adjuvant of chemotherapy.

5. REFERENCES

Amé, J.C., Rolli, V., Schreiber, V., Niedergang, C., Apiou, F., Decker, P., Muller, S., Höger, T., Ménisser-de Murcia, J., de Murcia, G. (1999). PARP-2, a novel mammalian DNA damage-dependent poly(ADP-ribose) polymerase. J. Biol. Chem. 247, 17860-17868.

Bryant, H.E., Schultz, N., Thomas, H.D., Parker, K.M., Flower, D., Lopez, E., Kyle, S., Meuth, M., Curtin, N.J., Helleday, T. (2005). Specific killing of BRCA2-deficient tumors with inhibitors of poly(ADP-ribose) polymerase. Nature 434, 913-917.

Cimmino, G., Pepe, S., Laus, G., Chianese, M., Prece, D., Penitente, R., Quesada, P. (2007). Poly(ADPR) polymerase-1 signaling of the DNA damaging induced by DNA topoisomerase I poison in D54 (p53wt) and U251 (p53mut) glioblastoma cell lines. Pharmacol. Res. 55, 49-56.

Davis, P.L., Shaiu, W.L., Scott, G.L., Iglehart, J.D., Hsieh, T.S., Marks, J.R. (1998). Complex response of breast epithelial cell to topoisomerase inhibitors. Anticancer Res. J. 18, 2919-2932.

Feeney, G.P., Errington, R.J., Wiltshire, M., Marquez, N., Chappel, S.C., Smith P.J. (2003). Tracking the cell cycle origins for escape from topotecan action by breast cancer cells. Br. J. Cancer 88, 1310-1317.

Gambi, N., Tramontano, F., Quesada, P. (2008). Poly(ADPR) polymerase inhibition and apoptosis induction in cDDP-treated human carcinoma cell lines. Biochem. Pharmacol. 75, 2356-2363.

Haince, J.F., Kozlov, S., Dawson, V.L., Dawson, T.M., Hendzel, M.J., Lavin, M.F., Poirier, G.G. (2007). Ataxia telangiectasia mutated (ATM) signaling network is modulated by a novel poly(ADP-ribose)-dependent pathway in the early response to DNA-damaging agents. J. Biol. Chem. 282, 16441-16453.

Haince, J.F., McDonald, D., Rodrigue, A., Déry, U., Masson, J.Y., Hendzel, M.J., Poirier, G.G. (2008). PARP-1-dependent kinetics of recruitment of MRE11 and NBS1 proteins to multiple DNA damage sites. J. Biol. Chem. 283, 1197-1208.

Hastak, K., Alli, E., Ford, J.M. (2010). Synergistic chemosensitivity of triple-negative breast cancer cell lines to PARP inhibition, gemcitabin and cisplatin. Caner Res [Epub ahead of print] PMID: 20798217.

Huber, A., Bai, P., de Murcia, J.M., de Murcia G. (2004). PARP-1, PARP-2, ATM in the DNA damage response: functional synergy in mouse development. DNA Repair 3, 1103-1108.

Khanna, K.K., Jackson, S.P. (2001). DNA double-strand breaks: signaling, repair and the cancer connection. Nat. Genet. 27, 247-254.

Malanga, M., Althaus, F.R. (2004). Poly(ADP-ribose) reactivates stalled DNA topoisomerase I and induces DNA strand break resealing. J. Biol. Chem. 279, 5244-5248.

Malanga, M., Althaus, F.R. (2005). The role of poly(ADP-ribose) in the DNA damage signalling network. Biochem. Cell. Biol. 83, 354-364.

Mortusewicz, O., Amé, J.C., Schreiber, V., Leonhardt, H. (2007). Feedback-regulated poly(ADP-ribosyl)ation by PARP-1 is required for rapid response to DNA damage in living cells. Nucleic Acids Res. 35, 7665-7675.

Pommier, Y. (2006). Topoisomerase I inhibitors: camptothecins and beyond. Nat. Rev. Cancer 6, 789-802.

Rodriguez-Hernandez, A., Brea-Calvo, G., Fernandez-Ayala, D.J.M., Cordero, M., Navas, P., Sanchez-Alcazar, J.A. (2006). Nuclear caspase-3 and caspase-7 activation, and Poly(ADP-ribose) polymerase cleavage are early events in camptothecin-induced apoptosis. Apoptosis 11, 131-139.

Roleau, M., Patel, A., Hendzel, M.J., Kaufmann, S.H., Poirer, G.G. (2010). PARP inhibitor: PARP-1 and beyond. Nat. Rev. Cancer 10, 293-301.

Sandhu, S.K., Yap, T.A., de Bono, J.S. (2010). Poly(ADP-ribose) polymerase inhibitors in cancer treatment: a clinical perspective. Eur. J. Cancer 46, 9-20.

Schreiber, V., Amé, J.C., Dollé, P., Schultz, I., Rinaldi, B., Fraulob, V., Ménissier-de Murcia, J., de Murcia G. (2002). Poly(ADP-ribose) polymerase-2 (PARP-2) is requie for efficient base excision DNA repair in association with PARP-1 and XRCC1. J. Biol. Chem. 277, 23028-23036.

Scovassi, A.I., Poirier, G.G. (1999). Poly(ADP-ribosyl)ation and apoptosis. Mol. Cell. Biochem. 199, 125-137.

Staker, B.L., Hjerrild, K., Feese, M.D., Behnke, C.A., Burgin, A.B. Jr, Stewart, L. (2002). The mechanism of topoisomerase I poisoning by a camptothecin analog. Proc. Natl. Acad. Sci. USA 99, 15387-15392.

Tentori, L, Muzi, A., Dorio, A.S., Scarsella, M., Leonetti, C., Shah, G.M., Xu, W., Camaioni, E., Gold, B., Pellicciari, R., Dantzer, F., Zhang, J., Graziani, G. (2010). Pharmacological inhibition of Poly(ADP-ribose) polymerase (PARP) activity in PARP-1 silenced tomor cells increases chemosensitivity to temozolomide and to a N3-Adenine selective methylating agent. Curr. Cancer Drug Targets. 10, 368-383.

Tentori, L., Graziani, G. (2005). Chemopotentiation by PARP inhibitors in cancer therapy. Pharmacol. Res. 53, 25-33.

Tomicic, M.T., Christmann, M., Kaina, B. (2005). Topotecan-triggered degradation of topoisomerase I is p53-dependent and impacts cell survival. Cancer Res. 65, 8920-8926.

Tuduri, S., Crabbé, L., Conti, C., Tourrière, H., Holtgreve-Grez, H., Jauch, A., Pantesco, V., De Vos, J., Thomas, A., Theillet, C., Pommier, Y, Tazi, J., Coquelle, A., Pasero, P. (2009). Topoisomerase I suppresses genomic instability by preventing interference between replication and transcription. Nat. Cell Bio. 11, 1315-1324.

Wang, M., Wu, W., Wu, W., Rosidi, B., Zhang, L., Wang, H., Iliakis, G. (2006). PARP-1 and Ku compete for repair of DNA double strand breaks by distinct NHEJ pathway. Nucleic Acids Res. 34, 6170-6182.

Yélamos, J., Schreiber, V., Dantzer, F. (2008). Toward specific functions of poly(ADP-ribose) polymerase-2. Mol. Med. 14, 169-178.

Biochemical Pharmacology xxx (2010) xxx–xxx

Contents lists available at ScienceDirect

Biochemical Pharmacology

journal homepage: www.elsevier.com/locate/biochempharm

Poly(ADP-ribose) polymerase signaling of topoisomerase 1-dependent DNA damage in carcinoma cells

Giovanna D'Onofrio [a], Filomena Tramontano [a], Annalisa Susanna Dorio [b], Alessia Muzi [b], Valeria Maselli [a], Domenico Fulgione [a], Grazia Graziani [b], Maria Malanga [a], Piera Quesada [a,*]

[a] Department of Structural and Functional Biology, University Federico II of Naples, Italy
[b] Department of Neuroscience, University of Rome Tor Vergata, Italy

ARTICLE INFO

Article history:
Received 30 July 2010
Received in revised form 17 September 2010
Accepted 20 September 2010
Available online xxx

Keywords:
Topotecan (TPT)
PARP-1 and -2
PJ34 Inhibitor
p53
Carcinoma cells

ABSTRACT

A molecular approach to enhance the antitumour activity of topoisomerase 1 (TOP1) inhibitors relies on the use of chemical inhibitors of poly(ADP-ribose)polymerases (PARP). Poly(ADP-ribosyl)ation is involved in the regulation of many cellular processes such as DNA repair, cell cycle progression and cell death. Recent findings showed that poly(ADP-ribosyl)ated PARP-1 and PARP-2 counteract camptothecin action facilitating resealing of DNA strand breaks. Moreover, repair of DNA strand breaks induced by poisoned TOP1 is slower in the presence of PARP inhibitors, leading to increased toxicity.

In the present study we compared the effects of the camptothecin derivative topotecan (TPT), and the PARP inhibitor PJ34, in breast (MCF7) and cervix (HeLa) carcinoma cells either PARP-1 proficient or silenced, both BRCA1/2$^{+/+}$ and p53$^{+/+}$.

HeLa and MCF7 cell lines gave similar results: (i) TPT-dependent cell growth inhibition and cell cycle perturbation were incremented by the presence of PJ34 and a 2 fold increase in toxicity was observed in PARP-1 stably silenced HeLa cells; (ii) higher levels of DNA strand breaks were found in cells subjected to TPT + PJ34 combined treatment; (iii) PARP-1 and -2 modification was evident in TPT-treated cells and was reduced by TPT + PJ34 combined treatment; (iv) concomitantly, a reduction of soluble/active TOP1 was observed. Furthermore, TPT-dependent induction of p53, p21 and apoptosis were found 24–72 h after treatment and were increased by PJ34 both in PARP-1 proficient and silenced cells. The characterization of such signaling network can be relevant to a strategy aimed at overcoming acquired chemoresistance to TOP1 inhibitors.

1. Introduction

The camptothecin derivative topotecan (TPT) is a DNA topoisomerase 1 (TOP1) inhibitor approved for the treatment of ovarian cancer, non small-cell lung cancer and under clinical investigation for a number of advanced solid tumours and haematological malignancies [1]. The drug reversibly abolishes the DNA religation activity of TOP1 generating single strand breaks (SSBs) to which the protein is covalently linked. Double strand breaks (DSBs) arise when replication forks collide with the SSBs and run off. Thus, TPT-induced DSBs are largely replication dependent or S phase specific [2,3].

Eukaryotes have two pathways for repairing DSBs: homologous recombination (HR) and non homologous end joining (NHEJ). The relative contribution of these two DSB repair pathways seems to differ depending on the cell cycle phase; HR acts mainly in the S and G2 phases, whereas NHEJ acts mainly in the G1 phase [4,5]. For these reasons, TPT-induced replication-dependent DSBs are usually repaired by the HR pathway [6].

Poly(ADP-ribosyl)ation is a post-translational modification catalyzed by poly(ADP-ribose)polymerase-1 and -2 (PARP-1 and PARP-2) and is one of the earliest cellular responses to DNA damage. PARP-1 and PARP-2 belong to a family of enzymes that cleave β-NAD$^+$ in nicotinamide and ADP-ribose to form long and branched (ADP-ribose) polymers (PAR) on glutamic acid residues within the primary sequence of PARP-1 and PARP-2 (automodification) and of other cellular proteins (heteromodification). This process causes chromatin decondensation around damage sites, recruitment of repair machineries, such as base excision repair complexes, and accelerates DNA damage repair [7,8]. In contrast, when DNA damage exceeds cell repair capacity PARP-1 undergoes cleavage by caspases into two fragments of 89 kDa and of 24 kDa, thereby avoiding futile cycling of PAR that would otherwise deplete the cell of β-NAD$^+$ required for the onset of apoptosis [9]. Moreover, interaction of PAR with the p53 oncoprotein is able to modulate its transcriptional activity [10].

* Corresponding author. Tel.: +39 081 679165.
E-mail address: quesada@unina.it (P. Quesada).

0006-2952/$ – see front matter © 2010 Elsevier Inc. All rights reserved.
doi:10.1016/j.bcp.2010.09.019

PARP-1 also affects DSBs repair as indicated by the increased sensitivity of PARP-1-deficient cells to DSBs inducing agents, especially to camptothecin [2]. Furthermore, the molecular mechanisms underlying tumour chemosensitization to TOP1 poisons by PARP inhibitors have been in part clarified by recent findings showing that poly(ADP-ribos)ylated PARP-1 and PARP-2 counteract camptothecin action facilitating resealing of DNA strand breaks [11]. This occurs through noncovalent yet specific interaction of PAR with particular TOP1 sites which results in inhibition of DNA cleavage and stimulation of the religation reaction [12]. Another mechanism proposed to explain the potentiation of camptothecin cytotoxicity by PARP inhibitors, is via the inhibition of base excision repair system, of which PARP-1 and -2 are important components. This model is supported by the association of tyrosyl phosphodiesterase-1, which removes the TOP1 cleavable complex, with base excision repair components that interact with PARP-1 [13].

Indeed, PARP-1 inhibition enhances the cytotoxic effects of TPT [14]. The potential of PARP inhibitors to increase the efficacy of chemotherapy has led to the development of a wide range of specific inhibitors – quinazolinone derivates – like NU1025 or PJ34 which display increased potency compared to the prototype 3-aminobenzamide (3-ABA) [15]. In this regard, we previously demonstrated a TPT-dependent PARP-1 activation in glioblastoma cells, while co-treatment with the PARP inhibitor NU1025 increased the TPT-dependent p53 up-regulation [16]. Moreover, we showed PJ34 chemo-potentiation of cisplatin in colon carcinoma cells [17].

It has been reported that PARP inhibitors would be particularly effective in BRCA1/2 mutated breast carcinoma cells [18]. In fact, PARP-1 and PARP-2 are required for the base excision repair pathway, whereas the BRCA proteins are critical for the HR pathway. Cells can survive when one repair system breaks down, but they start to die when both DNA repair mechanisms stop functioning.

Furthermore, a factor supposed to be involved in determining the sensitivity of cells to TOP1 inhibitors is p53. However, for breast cancer cells the p53 status was not found to be predictive of sensitivity to camptothecins [19].

On the basis of such evidences, we have investigated the role of PARP-1 in the DNA damage response to TOP1 inhibitors, in human BRCA1/2$^{+/+}$ and p53$^{+/+}$ mammary (MCF7) and cervix (HeLa) carcinoma cells treated with TPT as single agent or in association with a PARP inhibitor. Furthermore, TPT sensitivity of HeLa cells in which PARP-1 has been knocked down by RNA interference, has been compared to that of HeLa cells treated with the PARP inhibitor.

2. Materials and methods

2.1. Drugs, antibodies and chemicals

TPT was from Glaxo Smith-Kline (Verona, Italy) and PJ34 [N-(6-oxo-5,6,-dihydrophenanthridin-2-yl)-(N,N-dimethylamino)acetamide] from Alexis Biochemicals (Vinci-Biochem, Firenze, Italy). The cocktail of protease inhibitors was from ROCHE-Diagnostic (Milano, Italy).

Nicotinamide adenine [adenylate-^{32}P] dinucleotide-[^{32}P]-NAD^{+} (1000 Ci/mmol, 10 mCi/ml) was supplied by GE Healthcare (Milano, Italy).

Propidium iodide (PI) and RNAse were from Sigma–Aldrich (Milano, Italy).

PVDF (poly-vinylidene-fluoride) membrane was from MILLIPORE S.p.A. (Milano, Italy). Anti-PARP-1 mouse monoclonal antibody (F1–23) was from Alexis Biochemicals (Vinci-Biochem, Firenze, Italy) and anti-DNA TOP1 antibody from ABCAM, (Cambridge, UK). Anti-p53 (DO-1), anti-p21 (C-19), anti-BAX (P-19) and anti-GAPDH (H-2) mouse monoclonal antibodies were from Santa-Cruz Biotechnology (DBA, Milano, Italy); anti-actin (A2066) mouse monoclonal antibody and goat anti-mouse and goat anti-rabbit IgG HRP-conjugated antibodies were from Sigma–Aldrich (Milano, Italy). Anti-γH2AX (ser139, 2577) rabbit antibody was from Cell Signaling (Invitrogen Milano, Italy).

All other chemicals were of the highest quality commercially available.

2.2. Cell cultures

Cervix (HeLa) and mammary (MCF7) carcinoma cells were maintained in Dulbecco's modified eagle's medium (DMEM) containing 10% (v/v) heat-inactivated foetal bovine serum (FBS), 100 U/ml penicillin, 100 mg/ml streptomycin, 5 mM L-glutamine and incubated at 37 °C in a humidified atmosphere, plus 5% CO_2.

Stably PARP-1 silenced HeLa cells (hereafter referred to as HeLa$^{SiP\text{-}1}$) or transfected with the pBabe vector carrying the puromycin resistance gene (hereafter referred to as HeLa^{Babe}) were obtained as previously described [20].

2.3. Cell growth inhibition

MCF7 and HeLa cells were seeded at 1×10^5 cells; after 24 h, cell cultures were treated with graded concentrations of TPT and PJ34 and cell growth inhibition was assessed at different time points (24, 48, 72 h) using the 3-[4,5-dimethylthiazol-2-yl]-2,5-diphenyltetrazolium bromide (MTT) assay. All the experiments were performed in triplicate.

2.4. Cytofluorimetric analysis

Control and treated cells were detached by enzymatic treatment (trypsin/EDTA 0.02%), washed in PBS (w/o) Ca^{++}/Mg^{++} pooled with floating cells and recovered by centrifugation at 1200 rpm for 15 min at 4 °C. Cells were fixed in 70% ethanol and stored at −20 °C until analysis. After washing in PBS (w/o) Ca^{++}/Mg^{++}, cells were stained in 2 ml of propidium iodide (PI) staining solution [50 μg/ml of PI, 1 mg/ml of RNAse A in PBS (w/o) Ca^{++}/Mg^{++}, pH 7.4] overnight at 4 °C and DNA flow cytometry was performed in duplicate by a FACScan flow cytometer (Becton Dickinson Franklin Lakes, NJ, USA) coupled with a CICERO work station (Cytomation). Cell cycle analysis was performed by the ModFit LT software (Verity Software House Inc., Topsham, ME, USA). FL2 area versus FL2 width gating was done to exclude doublets from the G2/M region. For each sample 15,000 events were stored in list mode file.

2.5. Alkaline comet assay

Cells were suspended in PBS at a density of 10^4 cells/ml and mixed with an equal volume of fresh low-melting agarose (LMA, 1% in PBS); 80 μl of agarose cell suspension was spread on normal-melting agarose (NMA, 1% in PBS) slides and covered with a cover-slip. Two slides were prepared per sample. After gelling for 5 min on an ice bed, the cover-slip was gently removed and another layer was added, cover-slipped and allowed to solidify for 5 min on ice before gently removing the cover-slip. The slides were then immersed in a freshly prepared ice-cold lysis solution (2.5 M NaCl, 0.1 M Na_2EDTA, 0.01 M Tris, 1% Triton X-100, 10% DMSO, pH 10) for 1 h. The slides were drained and placed in a horizontal electrophoresis tank filled with freshly prepared alkaline buffer (0.3 M NaOH, 1 mM Na_2EDTA, pH 13). Electrophoresis was carried out in this buffer for 20 min at 300 mA. Finally, the slides were gently washed twice in a neutralization buffer (Tris–HCl 0.4 M, pH 7.5) for 5 min to remove alkali and detergent, and stained with

Please cite this article in press as: D'Onofrio G, et al. Poly(ADP-ribose) polymerase signaling of topoisomerase 1-dependent DNA damage in carcinoma cells. Biochem Pharmacol (2010), doi:10.1016/j.bcp.2010.09.019

50 μl/ml DAPI (3 h). Images of a minimum of hundred cells from each sample were analysed on a fluorescence microscope (Nikon Instruments S.p.A. Firenze, Italy); overlapping figures were avoided from each slide. Quantitative assessment of DNA damage was performed using Comet Score 1.5 Image Analysis (TriTek Corporation, Sumerduck, VA, USA) software which computes the integrated intensity profile for each cell. DNA damage was measured as olive tail moment [(tail mean − head mean) × % of DNA in the tail/100]. The results were analysed by Student's *t*-test and were considered statistically significant at $P < 0.008$.

2.6. Analysis of [^{32}P]-PAR synthesis

Following treatment with 10 μM TPT ± 5 μM PJ34 of intact cell (5×10^6 cells/plate), [^{32}P]-PAR synthesis was determined by substituting the culture medium with 1 ml of 56 mM HEPES buffer pH 7.5, containing 28 mM KCl, 28 mM NaCl, 2 mM $MgCl_2$, 0.01% digitonin, 0.1 mM PMSF, 1:25 dilution of a cocktail of protease inhibitors, 0.125 μM NAD^+ and 5 μCi [^{32}P]-NAD^+ (1000 Ci/mmol). After incubation at 37 °C for 30 min, cells were scraped off the plates, transferred to Eppendorf tubes and mixed with TCA at 20% (w:v) final concentration. After 15 min standing on ice, samples were collected by centrifugation at 1200 rpm for 15 min, washed twice with 5% TCA and three times with ethanol. [^{32}P]-PAR incorporated in the TCA-insoluble fraction was measured by Cerenkov counting using a LS8100 liquid scintillation spectrometer (Beckman Coulter S.p.A. Milano, Italy). Finally, TCA protein pellets were resuspended in Laemmli buffer; proteins were separated by 5–15% SDS-PAGE and after electroblotting on PVDF membrane, [^{32}P]-PAR acceptors were visualized by autoradiography. Immunodetection of specific proteins was accomplished on the same blots after autoradiography.

PJ34 efficiency as PARP inhibitor, was determined in an in vitro enzymatic activity assay using permeabilized cells: cell pellets were resuspended in 40 mM Tris–HCl pH 7.8, 0.6 mM EDTA, 30 mM $MgCl_2$, 0.05% Triton X-100, 1 mM β-mercaptoethanol, 20% glycerol, 1 mM PMSF and a 1:25 dilution of the cocktail of protease inhibitors. To maximally stimulate PAR synthesis, DNA strand breaks were induced by sonication for 30 s at medium intensity; finally, samples were incubated at 30 °C for 1 h with 5 μCi/ml [^{32}P]-NAD^+ and 50 μM unlabeled β-NAD^+, in the presence or absence of 5 μM PJ34.

Reactions were stopped by TCA addition (20% final concentration) and the samples were processed and analysed as described above.

2.7. Isolation of nuclear and post-nuclear fractions

To isolate sub-cellular fractions, cells were suspended in a buffer containing 30 mM Tris–HCl pH 7.5, 1.5 mM $MgCl_2$, 10 mM KCl, 1% (v/v) Triton X-100, 20% glycerol, 2 mM PMSF and the protease inhibitors cocktail solution. After 30 min of incubation on ice, cellular suspensions were centrifuged at 960 × *g* for 90 s at 4 °C and the nuclear fractions recovered in the pellet. The supernatant represents the post-nuclear fraction.

Nuclear fractions were resuspended in 20 mM HEPES pH 7.9, containing 20 mM KCl, 0.2 mM EDTA, 1.5 mM $MgCl_2$, 25% glycerol and the protease inhibitors cocktail solution. Protein concentration was determined using the Bradford protein assay reagent (BIO-RAD, Milano, Italy) with bovine serum albumin as a standard.

2.8. Autoradiographic and immunological analyses

Aliquots of 120 μg of cellular proteins were separated by SDS-PAGE (5–15% gradient gels) and transferred onto a PVDF membrane using an electroblotting apparatus (BIO-RAD). The membrane was subjected to autoradiographic analysis by the PhosphorImager (BIO-RAD) and/or to immunodetection after blocking with 5% non-fat milk in TBST 1 h, with anti-PARP-1 (F1–23; diluted 1:5000), anti-TOP1 (Scl-70; diluted 1:2500), anti-p53 (DO-1; diluted 1:5000), anti-p21 (C-19; diluted 1:1000), anti-Bax (P-19; diluted 1:500), anti-GAPDH (H2; diluted 1:5000), anti-γH2AX (2577; diluted 1:1000) and anti-actin (A2066; diluted 1:1000).

As secondary antibodies goat-anti-mouse or goat-anti-rabbit IgG HRP-conjugate (diluted 1:10,000–1:20,000) in 3% (w/v) non-fat milk in TBST were used. Peroxidase activity was detected using the ECL Advance Western blotting kit of GE Healthcare (Milano, Italy) and quantified using the Chemiluminescent detection system GS710 (BIO-RAD) and the Quantity One software: the arbitrary densitometric units were normalised on those of the GAPDH loading control.

3. Results

3.1. Effect of PJ34 on TPT-induced growth inhibition in human carcinoma cells

In preliminary experiments human cervical (HeLa) and mammary (MCF7) carcinoma cell lines showed comparable TPT-dependent growth inhibition, as measured by the MTT assay (data not shown). Furthermore, PARP-1 silencing by stable shRNA expression in HeLa cells (HeLa^{SiP-1}) rendered these cells more sensitive to the cytotoxic effects of the drug. In particular, while in a 72 h assay, 10 μM TPT for 1 h exerted mainly cytostatic effects in control cells (Hela^{Babe}), the same treatment caused 45% (±5) of PARP-1 silenced cells (HeLa^{SiP-1}) to die. In the presence of 5 μM PJ34 30% (±6) of PARP-1 proficient and 60% (±9) of PARP-1 deficient cells underwent cell death (data not shown).

To gain insight into the mechanism of enhanced TPT toxicity as a consequence of alteration of the cellular poly(ADP-ribosyl)ation status, we analysed cell cycle distribution at different recovery times after 1 h exposure to increasing concentrations of TPT, in the presence or absence of a functional PARP-1 (i.e., PARP-1 wild type HeLa or MCF7 cells versus HeLa^{SiP-1} cells). In another set of experiments, the PARP inhibitor PJ34 was used in combination with TPT, at a fixed concentration of 5 μM, maintained in the culture medium all over the recovery time. As shown in Fig. 1, as early as 24 h after treatment, graded concentrations of TPT induced a progressive increase of cell accumulation in the G2/M phase starting from 0.2 μM up to 1.25 μM. Higher TPT concentrations, instead, promptly arrested the cells in S phase.

The addition of the PARP inhibitor PJ34 to TPT concentrations <1.25 μM significantly increased G2/M cell accumulation, whereas when combined with ≥1.25 μM TPT concentrations, PJ34 induced S phase cell accumulation. As also shown in Fig. 1 cell cycle kinetics was unaffected by treatment of HeLa^{Babe} cells with PJ34 used as single agent.

HeLa^{SiP-1} cells treated with TPT concentrations comprised between 0.2 and 0.4 μM underwent a more pronounced increase of G2/M cell accumulation with respect to Hela^{Babe} cells exposed to the same concentrations of the TOP1 poison. Interestingly, 0.4 μM TPT caused in HeLa^{SiP-1} cells effects comparable to those observed in HeLa^{Babe} cells treated with 0.4 μM TPT plus the PARP inhibitor. However, PARP-1 silenced cells retained sensitivity to PJ34 and the combination 1.25 μM TPT + PJ34 caused S phase accumulation at a higher extent in HeLa^{SiP-1} than in Hela^{Babe} cells (Fig. 1).

Cytofluorimetric analyses at a longer recovery time (i.e., 72 h after treatment), revealed that alterations of the poly(ADP-ribosyl)ation system caused TPT to be cytotoxic at a concentration (1.25 μM) that was primarily cytostatic in control cells, as indicated by the appearance of a sub-diploid peak (apoptotic cells) both in PARP-1 silenced (HeLa^{SiP-1}) and PJ34-treated PARP-1 wild type cells (Hela^{Babe}) (Fig. 2). In this regard, the lack of

Please cite this article in press as: D'Onofrio G, et al. Poly(ADP-ribose) polymerase signaling of topoisomerase 1-dependent DNA damage in carcinoma cells. Biochem Pharmacol (2010), doi:10.1016/j.bcp.2010.09.019

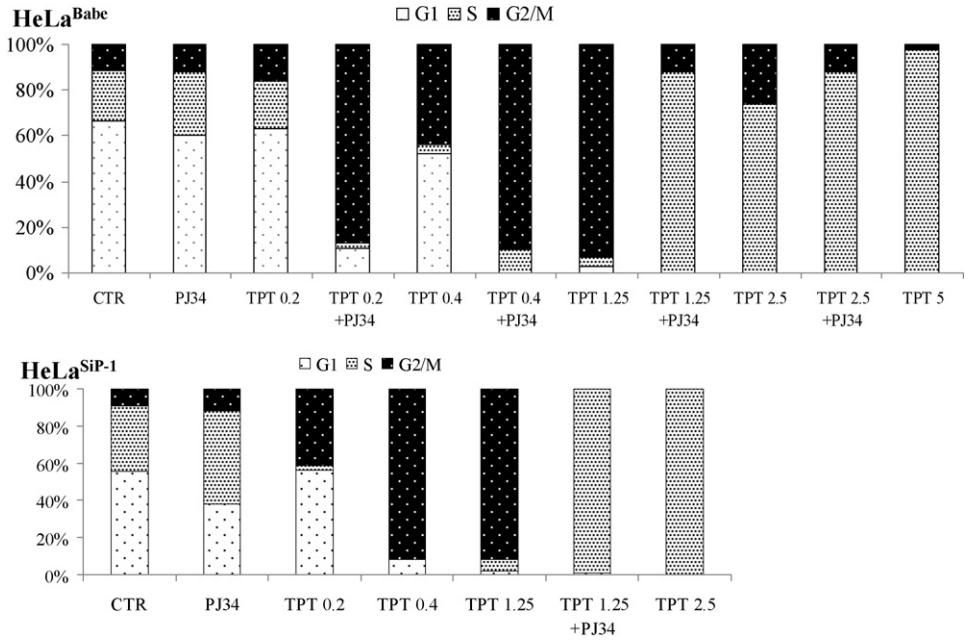

Fig. 1. Cell cycle analysis of HeLa^{Babe} and HeLa^{SiP-1} cells treated with TPT and PJ34 as single agents or in combination. Babe and SiP-1 cells were treated for 1 h with TPT (0.2–0.4–1.25–2.5–5 μM) in combination or not with PJ34 (5 μM) and left to recover for 24 h in fresh medium in the presence or absence of PJ34. The results are expressed as percentages of cells in the G1, S and G2/M phase of the cell cycle. Data refer to one out of three experiments giving similar results.

PARP-1 appeared to be more effective than PARP activity inhibition as the fraction of apoptotic cells was 62% in TPT-treated HeLa^{SiP-1} versus 38% in HeLa^{Babe}, subjected to a combined TPT + PJ34 treatment (Fig. 2).

3.2. Analysis of TPT and/or PJ34 dependent DNA damage in carcinoma cells

By alkaline comet assay, we analysed the level of both SSBs and DSBs [21] induced by 10 μM TPT ± PJ34 treatments. Fig. 3(A) shows that the olive tail moment determined for both HeLa (Babe and SiP-1) and MCF7 cells 24 h after 1 h treatment with TPT was increased in the cells left to recover in the presence of PJ34. The definition of a DSBs level was obtained by looking at the H2AX phosphorylation in isolated nuclei from Babe and SiP-1 cells. Fig. 3(B) shows that 72 h after 1 h treatment TPT induced a higher level of histone phosphorylation in HeLa^{SiP-1} than in Hela^{Babe} cells. H2AX phosphorylation was further incremented by PJ34 addition in both PARP-1 proficient and silenced cells.

3.3. Analysis of PAR synthesis in carcinoma cells after treatment with TPT ± PJ34

First, PJ34 efficacy as a PARP inhibitor at the concentration used in this study was assessed in an in vitro enzyme activity assay by incubating permeabilized and sonicated HeLa cells with exogenous 50 μM [^{32}P]-NAD$^+$ in the presence or absence of 5 μM PJ34. Sonication was performed to induce DNA strand breaks and

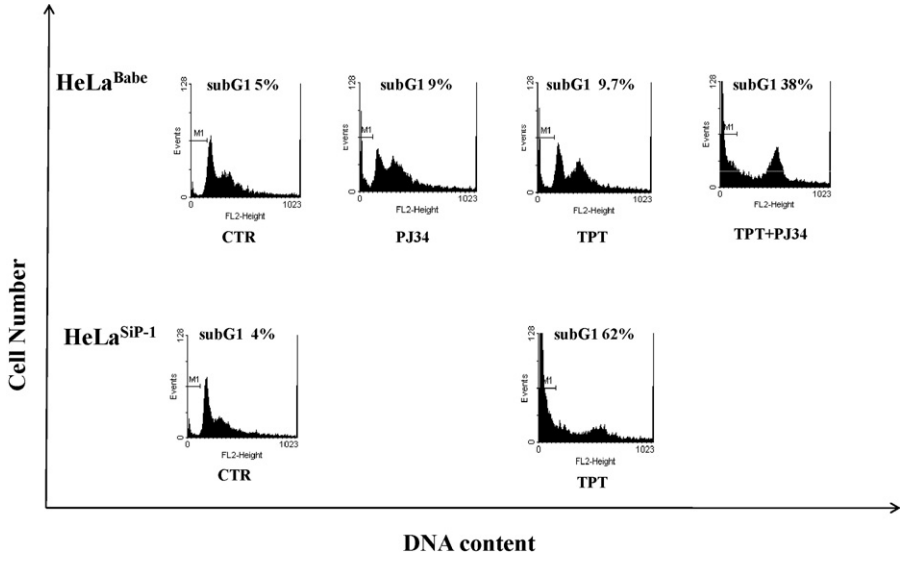

Fig. 2. Cell death analysis of HeLa cells subjected to TPT and PJ34 single and combined treatments. Babe and SiP-1 cells were treated for 1 h with 1.25 μM TPT in combination or not with 5 μM PJ34 and left to recover for 72 h in fresh medium in the presence or absence of PJ34. Flow cytometric determination of DNA content after PI staining is shown. The percentage of cells in the sub-diploid (subG1) peak is indicated. Data refer to one out of three experiments giving similar results.

Please cite this article in press as: D'Onofrio G, et al. Poly(ADP-ribose) polymerase signaling of topoisomerase 1-dependent DNA damage in carcinoma cells. Biochem Pharmacol (2010), doi:10.1016/j.bcp.2010.09.019

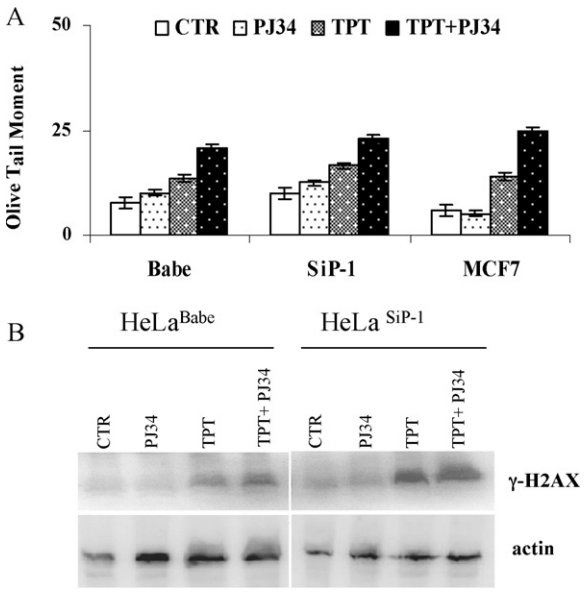

Fig. 3. DNA damage in HeLa^{Babe}, HeLa^{SiP-1} and MCF7 cells subjected to TPT ± PJ34 treatment. (A) Hundred cells 24 h after 1 h treatment with 10 μM TPT ± 5 μM PJ34 were analysed by alkaline comet assay on a fluorescence microscope (Nikon) and quantitative assessment of DNA damage was performed using Comet Score. The olive tail moment is reported as a mean of three different experiments ± S.E. (B) Western blot analysis of γH2AX levels in HeLa^{Babe} and HeLa^{SiP-1} cell nuclei treated 1 h with 10 μM TPT and allowed to recover in fresh medium in the presence or absence of 5 μM PJ34 for 72 h. Actin was used as loading control.

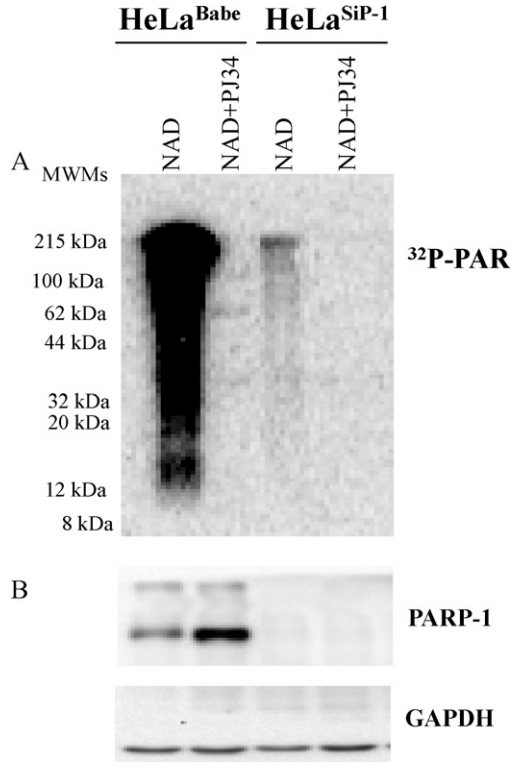

Fig. 4. PJ34-dependent inhibition of PAR synthesis in HeLa^{Babe} and HeLa^{SiP-1} cells. Cells were resuspended in lysis buffer, sonicated and incubated with 50 μM [^{32}P]-NAD$^+$ ± 5 μM PJ34 as described in Section 2. (A) Autoradiographic analysis of whole cell protein after SDS-PAGE and electroblot on PVDF. (B) Immunodetection of PARP-1 and GAPDH on the blot shown in (A).

thus maximally stimulate endogenous PARP activities. PAR synthesis on protein acceptors was analysed by SDS-PAGE followed by electroblotting onto PVDF membrane and autoradiography. As shown in Fig. 4(A), a high amount of protein-bound PAR was produced in HeLa cells and such an activity was completely inhibited by 5 μM PJ34. Although a wide range of modified proteins could be visualized, the main PAR acceptor was most likely PARP-1 as suggested by the strong radioactivity signal at the top of the gel and by the concomitant reduction of the PARP-1 immunoreactive band in the sample incubated with β-NAD$^+$ alone compared to that incubated with β-NAD$^+$ and PJ34 (Fig. 4(B)). Such a difference is explained by a band depletion due to the automodification-related electrophoretic mobility shift of a fraction of heavily poly(ADP-ribosylated) PARP-1. After quantification of immunoreactive bands by scanning densitometry and normalization of PARP-1 to GAPDH content it could be estimated that about 50% of PARP-1 underwent automodification.

The same kind of analysis carried out in HeLa^{SiP-1} cells, revealed a strongly reduced ADP-ribosylation capacity of these cells as a consequence of PARP-1 silencing (Fig. 4(A)): on the autoradiography only a light smear at the top of the gel could be visualized. As no PARP-1 could be detected in these cells by Western blotting (Fig. 4(B)) the modest ADP-ribosylation activity detected by the in vitro assay may be due to PARP-2 and/or other PARP.

Then, we used a different experimental setting to determine whether or not TPT could induce PARP(s) activation in intact cells. To this purpose, growing MCF7 cells were first exposed to the drugs and then PAR synthesis was measured in situ by incubation in the presence of 0.01% digitonin and 0.125 μM [^{32}P]-NAD$^+$. By autoradiography (Fig. 5(A)) we observed a main signal slightly up to PARP-1 molecular weight (113 kDa), indicating that DNA damage induced by TPT caused PARP-1 activation and automodification that was apparent already after 1 h treatment and further increased in the following 24 h recovery time. Such a trend was confirmed by scanning densitometry and normalization of data from autoradiography (Fig. 5(A)) to those relative to PARP-1 immunoreactive band (Fig. 5(B)). Minor autoradiographic bands were evident in the 90–50 kDa MWs range (Fig. 5(A)) indicating other PAR acceptors, possibly including other PARP. PARP-2 was detectable in this region as a 62 kDa protein band; a modification-related electrophoretic mobility shift could explain the lack of correspondence between the autoradiographic signal (Fig. 5(A)) and the PARP-2 immunoreactive band (Fig. 5(B)).

The autoradiographic signals were drastically reduced (up to 75% reduction) in cells co-treated with TPT and the PARP inhibitor with respect to cells treated with TPT as single agent.

Similar results were obtained in HeLa^{Babe} cells, while a [^{32}P]-PAR signal was undetectable in HeLa^{SiP-1} (data not shown).

3.4. Immunological analysis of PARP-1, TOP1, p53, p21 level in TPT ± PJ34 treated cells

By Western blotting we analysed changes in the endogenous levels of PARP-1, TOP1 and p53 in HeLa and MCF7 cells at different times (24, 48 and 72 h) after treatment with TPT ± PJ34.

Fig. 6 shows a comparable amount of PARP-1 in MCF7 cell samples at all time points, whereas the amount of soluble/active TOP1 was lowered (~50%) till 72 h after treatment with TPT alone or in combination with PJ34. Conversely, an up-regulation of p53 endogenous levels was evident until 72 h after treatment with TPT ± PJ34. Furthermore, the p53-dependent p21 induction was evidenced starting from 24 h after TPT treatment.

Fig. 7 shows that the amount of soluble/active TOP1 was drastically lowered also in HeLa cells (up to 70–80% reduction both in PARP-1 proficient and silenced cells) as a consequence of the treatments. Interestingly, such a decrease was sustained till 72 h after 1 h treatment.

Please cite this article in press as: D'Onofrio G, et al. Poly(ADP-ribose) polymerase signaling of topoisomerase 1-dependent DNA damage in carcinoma cells. Biochem Pharmacol (2010), doi:10.1016/j.bcp.2010.09.019

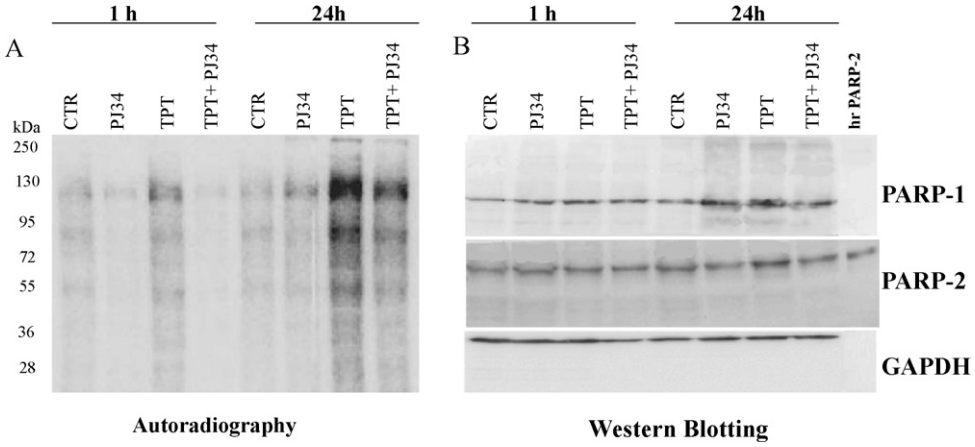

Fig. 5. TPT-dependent PARP activation in MCF7 cells. Following treatment with 10 μM TPT ± PJ34 and recovery for 24 h in fresh medium in the presence or absence of 5 μM PJ34, cells were incubated with 0.125 μM [^{32}P]-NAD$^+$, as described in Section 2. (A) Autoradiographic analysis of whole cell protein after SDS-PAGE and electroblot on PVDF. (B) Immunodetection of PARP-1, PARP-2 and GAPDH on the blot shown in (A). Fifty ng of human recombinant PARP-2 (hrPARP-2) was also loaded as a standard.

Again, we observed a TPT-dependent p53 up-regulation in both PARP-1 proficient and silenced cells, which appeared further increased by the use of PARP inhibitor (Fig. 7).

By densitometric scanning of immunoreactive bands we quantified the changes in p53 levels at different times after single and combined treatments. As shown in Fig. 8, the p53 level was 2–4 fold increased in HeLa^{Babe} cells 72 h after 1 h TPT ± PJ34 treatment. In HeLa^{SiP-1} cells a 10 fold increase was induced by TPT alone and this value increased (13 fold) in the presence of PJ34 during the recovery time.

Finally, 72 h after TPT treatment we analysed the expression of apoptotic markers. Fig. 9 shows in HeLa^{Babe} cells the caspase-dependent PARP-1 cleavage. In MCF7 cells, instead, the PARP-1 apoptotic fragment was hardly detectable but we observed the p53-dependent expression of BAX. Interestingly, we found that PJ34 was able to enhance both such apoptotic signals.

4. Discussion

The evaluation of PARP inhibitors as chemosensitizers is based on evidences linking PARP-1 and recently PARP-2, to the cellular DNA damage response [13]. This has led to the development of a multitude of potent inhibitors with various bioavailability and pharmacokinetic characteristics whose efficacy in the treatment of cancer in vivo has been evaluated in animal models [14,22]; several PARP inhibitors are currently under investigation in clinical trials [15,23]. However, a clear understanding of the mechanism(s) whereby PARP inhibitors potentiate the activity of antineoplastic agents is still lacking. Moreover, isoform specific PARP inhibitors are still missing while it is known that PARP-2 accounts for 10–20% of the total PARP activity in response to DNA damage [24 and references therein].

In our studies we used the hydrophilic PARP inhibitor PJ34 that has been recently reported to synergize with cisplatin in triple-negative breast cancer cells [25], in combination with the DNA TOP1 inhibitor, TPT. For our experiments we performed 1 h treatment with up to 10 μM TPT that was already reported to be sufficient for trapping TOP1 in MCF7 cells [26]. PJ34 was used at a concentration (5 μM) that was capable of inhibiting PARP activity but devoid of cytotoxic effects we found that TPT toxicity was higher when PAR synthesis was strongly reduced by either PARP-1 silencing (HeLa^{Sip-1} cells) or PJ34 administration (both in HeLa and MCF7 cells).

MCF7 and HeLa cells, according with their comparable PARP-1$^{+/+}$ BRCA1/2$^{+/+}$ and p53$^{+/+}$ status showed the same sensitivity to TPT, which determined a cell cycle arrest until 72 h after treatment. However, in combination with PJ34, TPT was cytotoxic even at a very low concentration (1.25 μM). Accordingly, 1.25 μM TPT alone was cytotoxic in PARP-1 silenced cells (HeLa^{SiP-1}). Nevertheless, the PARP inhibitor further increased the sensitivity of SiP-1 cells with respect to PARP-1 proficient cells treated with the drug combination, suggesting a PARP-2 involvement in the signaling of TPT-dependent DNA damage.

Consistently with the idea that poly(ADP-ribosyl)ation plays a role in the response to TPT-induced DNA damage, we found

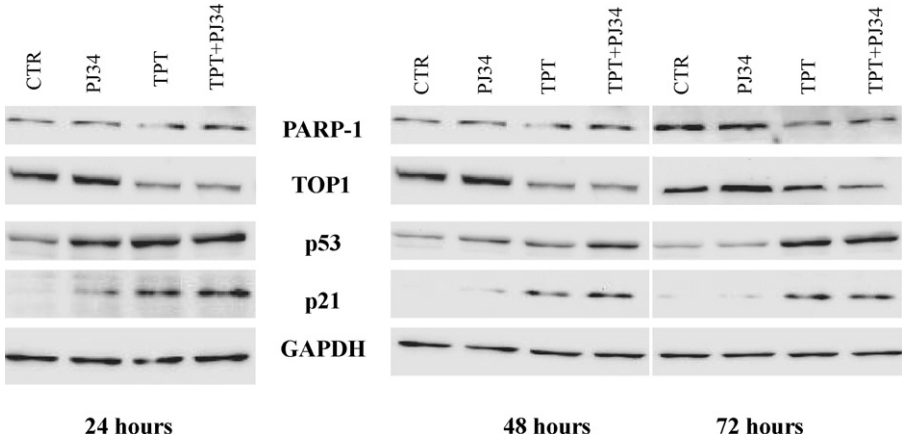

Fig. 6. Western blot analysis of PARP-1, TOP1, p53 and p21 in MCF7 cells. Cells were treated with 10 μM TPT for 1 h and allowed to recover in fresh medium in the presence or absence of 5 μM PJ34 for the indicated times. GAPDH was used as loading control.

Please cite this article in press as: D'Onofrio G, et al. Poly(ADP-ribose) polymerase signaling of topoisomerase 1-dependent DNA damage in carcinoma cells. Biochem Pharmacol (2010), doi:10.1016/j.bcp.2010.09.019

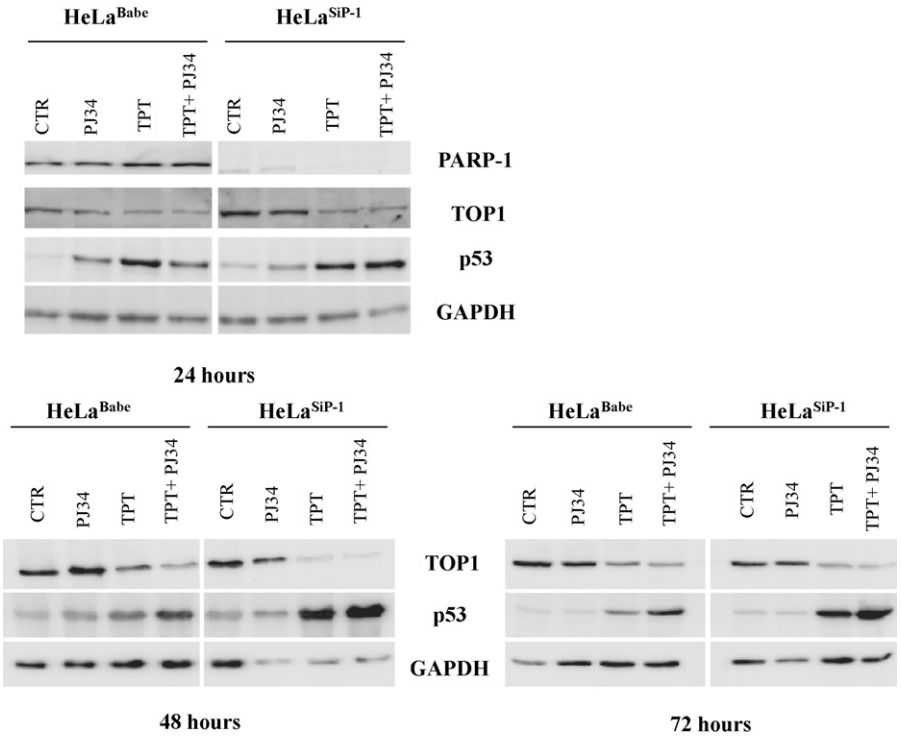

Fig. 7. Western blot analysis of PARP-1, TOP1, p53 and p21 in HeLa^{Babe} and HeLa^{SiP-1} cells. Cells were treated with 10 μM TPT for 1 h and allowed to recover in fresh medium in the presence or absence of 5 μM PJ34 for the indicated times. GAPDH was used as loading control.

increased PAR synthesis following cell exposure to 10 μM TPT. The PARP inhibitor PJ34 prevented PARP activity and concomitantly caused intensification of cell cycle perturbations and increased DNA damage.

In particular, we observed distinct cell cycle perturbation effects depending on the concentration of the TOP1 inhibitor and on the association with the PARP inhibitor: in the low TPT dose range, PJ34 in combination with 0.2–0.4 μM TPT caused more cells to be arrested in the G2/M phase, whereas combined with 1.25 μM TPT it arrested at the S phase cells that escaped TPT action. Furthermore, the G2/M block induced by 0.4 μM TPT in PARP-1 wild type cells was magnified in PARP-1 silenced HeLa cells. These evidences agree with the concept that after 1 h pulse (whatever the dose) of TPT not all the cells are prevented from entry in mitosis and then G2 cell lineages could survive TPT-mediated cytotoxicity [27]. Therefore, accumulation at the G2/M phase of tumour cells that escaped TPT action, provoked by PARP inhibition or by PARP-1 silencing, can be seen as a mechanism to overcome resistance to camptothecin derivatives. Interestingly, in PARP-1 silenced HeLa cells PJ34 increased the TPT S phase arrest as a further indication of PARP-2 implication.

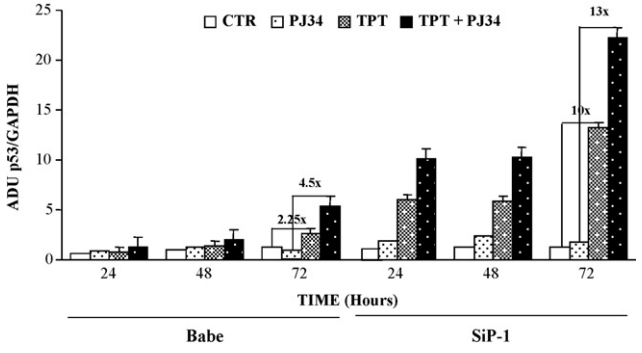

Fig. 8. Densitometric analysis of p53 levels in HeLa cell samples. After immunodetection on Western blots, band intensities were quantified by scanning densitometry. Data, expressed as arbitrary densitometric units (ADU), were normalized to the internal control GAPDH. Shown are the mean of three different experiments ± S.E.

Consistently, the TPT-dependent DNA damage level was increased by co-treatment with PJ34 both in PARP-1 proficient and PARP-1 silenced cells 24 h after treatment. In nuclei of such cells, differences in γH2AX levels deriving from TPT ± PJ34, also support PARP-1 and -2 stimulation of TPT-dependent DSBs repair.

Moreover, we found a sustained PAR synthesis from 1 to 24 h after treatment and most of the newly synthesized polymer was linked to PARP-1 itself. Two other PAR acceptors in the 55–95 kDa MW's range appeared to be TPT- and PJ34-dependent. Accordingly with the magnified effects of TPT + PJ34 treatment in PARP-1 silenced cells the PARP-2 modification could represent the mechanism of its participation in DSBs signaling and HR repair [24].

Indeed, these evidences suggest that the lack of PAR synthesis, by interfering with the repair of TOP1-induced DNA damage, causes DNA strand breaks accumulation and further delays cell cycle progression. Moreover, we found that TPT-treated cells entered the apoptotic program as a consequence of PARP-1 silencing and/or PARP inhibition.

The last set of results was based on mechanistic investigations addressed to show the long-term response to TPT action: after 1 h TPT pulse TOP1 soluble/active fraction was drastically reduced for at least 3 cell duplication cycles and p53/p21 levels increased within the same time frame. Such an up-regulation was even higher in cells lacking PARP-1 and further increased by TPT + PJ34 treatment, supporting again the involvement of PARP-2 in the signaling of TPT-dependent DNA damage.

These results are in agreement with those previously reported in the same cells treated with the methylating agent temozolomide in combination with the PARP inhibitor GPI 15427, suggesting the involvement of PARP-2 (or other PARP) in the repair of DNA damage provoked by temozolomide [20].

Please cite this article in press as: D'Onofrio G, et al. Poly(ADP-ribose) polymerase signaling of topoisomerase 1-dependent DNA damage in carcinoma cells. Biochem Pharmacol (2010), doi:10.1016/j.bcp.2010.09.019

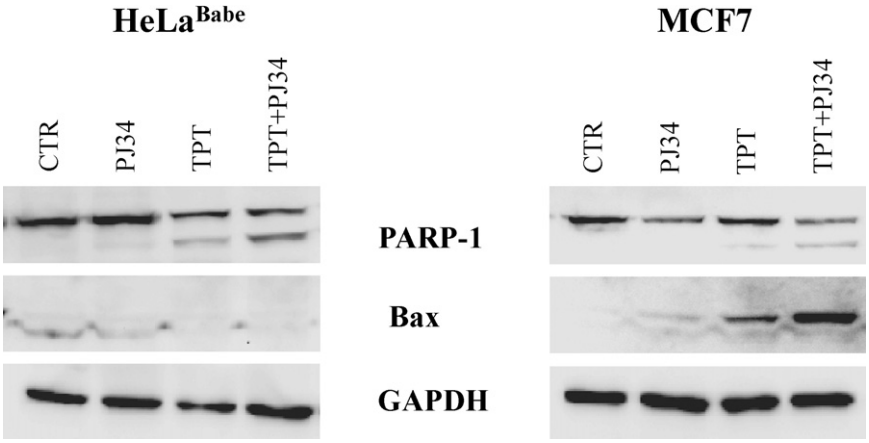

Fig. 9. Western blot analysis of PARP-1 and BAX in HeLa and MCF7 cells. Cells were treated with 10 μM TPT for 1 h and allowed to recover in fresh medium in the presence or absence of PJ34 for 72 h. GAPDH was used as loading control.

Our data also suggest a synergistic interaction of PARP-1 and PARP-2 with p53 in tumour suppression through their role in DNA damage response and genome integrity surveillance. Another study showed that in MCF7 cells inhibition of endogenous PARP-1 function suppresses the transactivation function of p53 in response to ionizing radiation [28]. We also observed that p53-dependent BAX expression and caspase-dependent PARP-1 proteolysis were sustained by the PARP inhibitor as a result of apoptosis induction.

By the all of such evidences we envisaged a TPT-dependent DNA damage signaling network, involving PARP. Indeed, the DNA damage arising from the trapping of TOP1 was signaled by PARP-1 and -2 and gathered by effectors like p53 and p21. Previous results suggest that p53 causes resistance of cells to TPT [29]. Our findings suggest a PARP modification induced by TPT-dependent DNA damage, while PARP-1 and -2 inactivation switches on p53/p21 pro-apoptotic role.

Indeed, caspase-dependent PARP-1 proteolysis contributes to restoring the apoptotic program in neoplastic cells. Nuclear caspases-mediated PARP-1 cleavage has been described in camptothecin-induced apoptosis as an early event that precedes the release of cytochrome c and AIF, generally thought to activate the chemotherapy-induced apoptosis by DNA-damaging drugs [30].

In conclusion, our findings contribute to the understanding of the molecular events triggered by TOP1 poison-dependent genomic damage and provide a rationale for the development of new approaches to sensitize cancer cells to chemotherapy.

Acknowledgement

This work was supported by funding from the Italian Ministry of Education and Research "Programmi di Ricerca Scientifica di Rilevante Interesse Nazionale" (PRIN 2007–2009).

References

[1] Pommier Y. Topoisomerase I inhibitors: camptothecins and beyond. Nat Rev Cancer 2006;6:789–802.
[2] Staker BL, Hjerrild K, Feese MD, Behnke CA, Burgin Jr AB, Stewart L. The mechanism of topoisomerase I poisoning by a camptothecin analog. Proc Natl Acad Sci USA 2002;99:15387–92.
[3] Pommier Y, Redon C, Rao VA, Seiler JA, Sordet O, Takemura H, et al. Repair of and checkpoint response to topoisomerase I-mediated DNA damage. Mutat Res 2003;532:173–203.
[4] Takata M, Sasaki MS, Sonoda E, Morrison C, Hashimoto M, Utsumi H, et al. Homologous recombination and non-homologous end-joining pathways of DNA double strand break repair have overlapping roles in the maintenance of chromosomal integrity in vertebrate cells. EMBO J 1998;17:5497–508.
[5] Essers J, van Steeg H, de Wit J, Swagemakers SM, Vermeij M, Hoeijmakers JH, et al. Homologous and non-homologous recombination differentially affect DNA damage repair in mice. EMBO J 2000;19:1703–10.
[6] Arnaudeau C, Lundin C, Helleday T. DNA double-strand breaks associated with replication forks are predominantly repaired by homologous recombination involving an exchange mechanism in mammalian cells. J Mol Biol 2001;307:1235–45.
[7] Burkle A. Poly(ADP-ribosyl)ation. LANDES Biosci 2005.
[8] Schreiber V, Dantzer F, Ame JC, de Murcia G. Poly(ADPribose): novel function for an old molecule. Nat Rev Mol Cell Biol 2006;7:517–28.
[9] Scovassi AI, Poirier GG. Poly(ADP-ribosyl)ation and apoptosis. Mol Cell Biochem 1999;199:125–37.
[10] Malanga M, Pleschke JM, Kleczkowska HE, Althaus FR. Poly(ADP-ribose) binds to specific domains of p53 and alters its DNA binding functions. J Biol Chem 1998;273(19):11839–43.
[11] Malanga M, Althaus FR. The role of poly(ADP-ribose) in the DNA damage signaling network. Biochem Cell Biol 2005;83(3):354–64.
[12] Malanga M, Althaus FR. Poly(ADP-ribose) reactivates stalled DNA topoisomerase I and induces DNA strand break resealing. J Biol Chem 2004;279(7):5244–8.
[13] Smith LM, Willmore E, Austin CA, Curtin NJ. The novel poly(ADP-Ribose) polymerase inhibitor, AG14361, sensitizes cells to topoisomerase I poisons by increasing the persistence of DNA strand breaks. Clin Cancer Res 2005;11:8449–57.
[14] Tentori L, Graziani G. Chemopotentiation by PARP inhibitors in cancer therapy. Pharmacol Res 2005;52:25–33.
[15] Sandhu SK, Yap TA, de Bono JS. Poly(ADP-ribose) polymerase inhibitors in cancer treatment: a clinical perspective. Eur J Cancer 2010;46(1):9–20.
[16] Cimmino G, Pepe S, Laus G, Chianese M, Prece D, Penitente R, Quesada P. Poly(ADPR)polymerase-1 signalling of the DNA damage induced by DNA topoisomerase I poison in D54(p53wt) and U251(p53mut) glioblastoma cell lines. Pharmacol Res 2007;55(1):49–56.
[17] Gambi N, Tramontano F, Quesada P. Poly(ADPR)polymerase inhibition and apoptosis induction in cDDP-treated human carcinoma cell lines. Biochem Pharmacol 2008;75(12):2356–63.
[18] Bryant HE, Schultz N, Thomas HD, Parker KM, Flower D, Lopez E, et al. Specific killing of BRCA2-deficient tumours with inhibitors of poly(ADP-ribose) polymerase. Nature 2005;434(7035):913–7.
[19] Davis PL, Shaiu WL, Scott GL, Iglehart JD, Hsieh TS, Marks JR. Complex response of breast epithelial cell lines to topoisomerase inhibitors. Anticancer Res J 1998;18(4C):2919–32.
[20] Tentori L, Muzi A, Dorio AS, Scarsella M, Leonetti C, Shah GM, et al. Pharmacological inhibition of Poly(ADP-ribose) polymerase (PARP) activity in PARP-1 silenced tumour cells increases chemosensitivity to temozolomide and to a N3-adenine selective methylating. Agent Curr Cancer Drug Targets 2010;10(4):368–83.
[21] Tice RR, Agurell E, Anderson D, Burlinson B, Hartmann A, Kobayashi. et al. Single cell gel/comet assay: guidelines for in vitro and in vivo genetic toxicology testing. Environ Mol Mutagen 2000;35:206–21.
[22] Giansanti V, Donà F, Tillhon M, Scovassi AI. PARP inhibitors: new tools to protect from inflammation. Biochem Pharmacol 2010. Apr 22 [Epub ahead of print] PMID: 20417190.
[23] Rouleau M, Patel A, Hendzel MJ, Kaufmann SH, Poirier GG. PARP inhibition: PARP1 and beyond. Nat Rev Cancer 2010;10:293–301.
[24] Yelamos J, Schreiber V, Dantzer F. Toward specific functions of poly(ADP-ribose) polymerase-2. Trends Mol Med 2008;14(4):169–78.
[25] Hastak K, Alli E, Ford JM. Synergistic chemosensitivity of triple-negative breast cancer cell lines to PARP inhibition, gemcitabine and cisplatin. Cancer Res 2010. Aug 26 [Epub ahead of print] PMID: 20798217.
[26] Feeney GP, Errington RJ, Wiltshire M, Marquez N, Chappell SC, Smith PJ. Tracking the cell cycle origins for escape from topotecan action by breast cancer cells. Br J Cancer 2003;88(8):1310–7.

Please cite this article in press as: D'Onofrio G, et al. Poly(ADP-ribose) polymerase signaling of topoisomerase 1-dependent DNA damage in carcinoma cells. Biochem Pharmacol (2010), doi:10.1016/j.bcp.2010.09.019

[27] Tuguri S, Crabbé L, Conti C, Tourrière H, Holtgreve-Grez H, Jauch A, et al. Topoisomerase I suppresses genomic instability by preventing interference between replication and transcription. Nat Cell Biol 2009;11(11): 1315–24.
[28] Wieler S, Gagné JP, Vaziri H, Poirier GG, Benchimol S. Poly(ADP-ribose) polymerase-1 is a positive regulator of the p53-mediated G1 arrest response following ionizing radiation. J Biol Chem 2003;278:18914–21.
[29] Tomicic MT, Christmann M, Kaina B. Topotecan-triggered degradation of topoisomerase I is p53-dependent and impacts cell survival. Cancer Res 2005;65(19):8920–6.
[30] Rodrıguez-Hernandez A, Brea-Calvo G, Fernandez-Ayala DJM, Cordero M, Navas P, Sanchez-Alcazar JA. Nuclear caspase-3 and capase-7 activation, and poly(ADP-ribose) polymerase cleavage are early events in camptothecin-induced apoptosis. Apoptosis 2006;11:131–9.

Please cite this article in press as: D'Onofrio G, et al. Poly(ADP-ribose) polymerase signaling of topoisomerase 1-dependent DNA damage in carcinoma cells. Biochem Pharmacol (2010), doi:10.1016/j.bcp.2010.09.019